

# Satellite Kinematics II: The Halo Mass-Luminosity Relation of Central Galaxies in SDSS

Surhud More<sup>1</sup> <sup>\*</sup>, Frank C. van den Bosch<sup>1</sup>, Marcello Cacciato<sup>1</sup>, H. J. Mo<sup>2</sup>,  
 Xiaohu Yang<sup>3</sup>, Ran Li<sup>2,4</sup>

<sup>1</sup>Max Planck Institute for Astronomy, Koenigstuhl 17, D69117, Heidelberg, Germany

<sup>2</sup>Department of Astronomy, University of Massachusetts, Amherst, MA 010039305, USA

<sup>3</sup>Shanghai Astronomical Observatory, Nandan Road 80, Shanghai 200030, China

<sup>4</sup>Department of Astronomy, Peking University, Beijing 100871, China

## ABSTRACT

The kinematics of satellite galaxies reflect the masses of the extended dark matter haloes in which they orbit, and thus shed light on the mass-luminosity relation (MLR) of their corresponding central galaxies. In this paper we select a large sample of centrals and satellites from the Sloan Digital Sky Survey (SDSS) and measure the kinematics (velocity dispersions) of the satellite galaxies as a function of the *r*-band luminosity of the central galaxies. Using the analytical framework presented in Paper I, we use these data to infer *both* the mean and the scatter of the MLR of central galaxies, carefully taking account of selection effects and biases introduced by the stacking procedure. As expected, brighter centrals on average reside in more massive haloes. In addition, we find that the scatter in halo masses for centrals of a given luminosity,  $\sigma_{\log M}$ , also increases with increasing luminosity. As we demonstrate, this is consistent with  $\sigma_{\log L}$ , which reflects the scatter in the conditional probability function  $P(L_c|M)$ , being independent of halo mass. Our analysis of the satellite kinematics yields  $\sigma_{\log L} = 0.16 \pm 0.04$ , in excellent agreement with constraints from clustering and group catalogues, and with predictions from a semi-analytical model of galaxy formation. We thus conclude that the amount of stochasticity in galaxy formation, which is characterized by  $\sigma_{\log L}$ , is well constrained, is independent of halo mass, and is in good agreement with current models of galaxy formation.

**Key words:** galaxies: haloes — galaxies: kinematics and dynamics — galaxies: fundamental parameters — galaxies: structure — dark matter — methods: statistical

## 1 INTRODUCTION

According to the standard framework of galaxy formation, dark matter haloes form gravitational potential wells in which baryons collapse, dissipate their energy and form stars and galaxies (White & Rees 1978; Blumenthal et al. 1984). The complex process of galaxy formation and evolution is believed to be governed by the mass of the dark matter halo in which it occurs. To understand the halo mass dependence of this process, it is important to statistically relate the observable properties (e.g. luminosity) of galaxies to the masses of their dark matter haloes.

The dark matter halo is bigger in extent than the visible matter in a galaxy due to the inability of dark matter to lose energy via dissipative processes. Therefore, a tracer

population, distributed over large distances from the center of the halo is necessary to reliably measure the mass of a dark matter halo. Satellite galaxies satisfy this requirement and their kinematics reflect the depth of the potential well they orbit. However, a reliable measurement of the kinematics requires a large number of satellites. Whereas a relatively large number of satellites can be detected in cluster-sized haloes, only a handful of satellites can be detected in less massive haloes. This leads to a large uncertainty on the kinematic measurement for less massive haloes. However, under the assumption that central galaxies of similar properties reside in similar mass haloes, one can stack such central galaxies and use their satellites to obtain a statistical measure of the kinematics even in low mass haloes. (Erickson, Gottesman & Hunter 1987; Zaritsky et al. 1993; Zaritsky & White 1994; Zaritsky et al. 1997).

During the past few years, data from large galaxy redshift surveys such as the Sloan Digital Sky Survey (SDSS;

<sup>\*</sup> International Max Planck Research School fellow  
 Email: more@mpia.de

York et al. 2000) and the Two degree Field Galaxy Redshift Survey (2dFGRS; Colless et al. 2001) has become available. The kinematics of satellite galaxies selected from these large datasets have been used to infer the mass-luminosity relationship (hereafter MLR) of central galaxies (McKay et al. 2002; Brainerd & Specian 2003; Prada et al. 2003; van den Bosch et al. 2004; Conroy et al. 2005, 2007) and to study the density profiles of dark matter haloes (Prada et al. 2003; Klypin & Prada 2007). These studies consistently find that the velocity dispersion of satellites (and hence the mass of the halo) increases with the luminosity of the central galaxy. However, Norberg, Frenk & Cole (2008, hereafter N08) demonstrated a quantitative disagreement in the results of these studies and showed that this disagreement is largely due to subtle differences in the selection criteria used to identify central and satellite galaxies. Therefore, it is crucial to understand how selection effects bias the MLR of central galaxies inferred from satellite kinematics.

The MLR of central galaxies is specified in terms of the conditional probability  $P(M|L_c)$ , which describes the probability for a central galaxy with luminosity  $L_c$  to reside in a halo of mass  $M$ . For a completely deterministic relation between halo mass and central luminosity,  $P(M|L_c) = \delta(M - M_0)$ , where  $\delta$  denotes the Dirac-delta function and  $M_0$  is a characteristic halo mass corresponding to centrals of luminosity  $L_c$ . The velocity dispersion,  $\sigma(L_c)$ , measured by stacking centrals with luminosity  $L_c$ , then translates into a mass  $M_0$  according to the scaling relation  $\sigma^3 \propto M$ . However, galaxy formation is a stochastic process and the distribution  $P(M|L_c)$  is expected to have non-zero scatter. If this scatter is appreciable then the stacking procedure results in combining the kinematics of haloes spanning a wide range in halo mass. This complicates the interpretation of the velocity dispersion. We addressed this issue in More, van den Bosch & Cacciato (2008; hereafter Paper I), where we investigated a method to measure both the mean and the scatter of the MLR of central galaxies using satellite kinematics. We outlined two different weighting schemes to measure the velocity dispersion of satellites, *satellite-weighting* and *host-weighting*, and showed that the mean and the scatter of the MLR can be inferred by modelling the velocity dispersion measurements in these two schemes simultaneously. In this paper, we apply this method to the spectroscopic galaxy catalogue from SDSS (Data Release 4) in order to determine both the mean and the scatter of the MLR of central galaxies.

The aim of this paper is twofold. First, we carry out a series of tests on a realistic mock galaxy catalogue to validate our method to infer the MLR of central galaxies from a redshift survey using satellite kinematics. In particular, we show that our central-satellite selection criterion and the method to measure the kinematics reliably recovers the true kinematics present in the mock catalogue. We also show that the mean and the scatter of the MLR inferred from the kinematics match the corresponding true relations in the mock catalogue. Second, we repeat the analysis on galaxies from the SDSS. In particular, we show that both the mean and the scatter of the MLR increase with the luminosity of the central galaxy. This demonstrates that the scatter in halo masses is non-negligible and must be taken into account when interpreting measurements involving stacking.

This paper is organized as follows. In Section 2 we describe the construction of the mock catalogue that is used to test our method of analysis. In Section 3 we briefly outline the iterative selection criterion used to select centrals and satellites. In Section 4 we describe and test the method used to measure the kinematics of satellites as a function of the central luminosity. The inference of the MLR from the kinematics of satellite galaxies requires the knowledge of the number density distribution of satellites within a halo. In Section 5 we show that this distribution can also be inferred from the selected satellites. In Section 6 we describe our model to interpret the measured velocity dispersions and show that this model is able to recover the true mean and scatter of the MLR of central galaxies from the mock catalogue. In Section 7 we apply our analysis method to a volume limited sample from SDSS and discuss the results. We summarize our results in Section 8.

## 2 MOCK CATALOGUES

It is important to carefully identify central and satellite galaxies from a redshift survey in order to study the kinematics of satellite galaxies. Furthermore, it is also important to reliably quantify the kinematics of the selected satellites as a function of central luminosity which in turn can yield the MLR of central galaxies. We monitor the performance of our method of analysis for each of these tasks using a realistic mock galaxy catalogue (MGC) which serves as a control dataset. The halo occupation of galaxies in the MGC is known a priori, thereby allowing an accurate assessment of the level of contamination of the selected sample of centrals and satellites due to false identifications and also a comparison between the kinematics recovered from the selected satellites and the actual kinematics present in the MGC.

The two essential steps to construct a MGC are to obtain a distribution of dark matter haloes and to use a recipe to populate the dark matter haloes with galaxies. For the former purpose, we use a numerical simulation of dark matter particles in a cosmological setup. For the latter, we use the conditional luminosity function (CLF) which describes the average number of galaxies with luminosities in the range  $L \pm dL/2$  that reside in a halo of mass  $M$ .

A distribution of dark matter haloes is obtained from a  $N$ -body simulation for a  $\Lambda$ CDM cosmology with parameters,  $\Omega_m = 0.238$ ,  $\Omega_\Lambda = 0.762$ ,  $\sigma_8 = 0.75$ ,  $n_s = 0.95$ ,  $h = H_0/100 \text{ km s}^{-1} \text{ Mpc}^{-1} = 0.73$ . The simulation consists of  $N = 512^3$  particles within a cube of side  $L_{\text{box}} = 300h^{-1}\text{Mpc}$  with periodic boundary conditions. The particle mass is  $1.33 \times 10^{10} h^{-1} M_\odot$ . Dark matter haloes are identified using the friends-of-friends algorithm (Davis et al. 1985) with a linking length of 0.2 times the mean inter-particle separation. Haloes obtained with this linking length have a mean overdensity of 180 (Porciani, Dekel & Hoffman 2002). We consider only those haloes which have at least 20 particles or more.

To populate the dark matter haloes with galaxies, we need to know the number and the luminosities of galaxies to be assigned to each halo. Furthermore, we also need to assign phase space coordinates to each of these galaxies. We use the CLF described in Cacciato et al. (2008) for the first purpose. The CLF is a priori split into a contribution from

centrals and satellites, i.e.  $\Phi(L|M) = \Phi_c(L|M) + \Phi_s(L|M)$ . Here,  $\Phi_c(L|M)dL$  denotes the conditional probability that a halo of mass  $M$  harbours a central galaxy of luminosity between  $L$  and  $L+dL$ , and  $\Phi_s(L|M)dL$  denotes the average number of satellites of luminosity between  $L$  and  $L+dL$ . The parameters that describe the CLF are constrained using the luminosity function (Blanton et al. 2005) and the luminosity dependence of the correlation length of galaxies (Wang et al. 2007a) in SDSS.

Let us consider a halo of mass  $M$ . The luminosity of the central galaxy within this halo is sampled from the distribution  $\Phi_c(L|M)$ . The average number of satellites that have a luminosity greater than  $L_{\min} = 10^9 h^{-2} L_\odot$  and reside within haloes of mass  $M$  is given by

$$\langle N_{\text{sat}} \rangle(M) = \int_{L_{\min}}^{\infty} \Phi_s(L|M) dL. \quad (1)$$

We assume Poisson statistics for the occupation number of satellites (Kravtsov et al. 2004; Yang et al. 2005a; Yang, Mo & van den Bosch 2008) and assign  $N_{\text{sat}}$  galaxies to the halo where  $N_{\text{sat}}$  is drawn from

$$P(N_{\text{sat}}|M) = \exp(-\mu) \frac{\mu^{N_{\text{sat}}}}{N_{\text{sat}}!}, \quad (2)$$

with  $\mu = \langle N_{\text{sat}} \rangle(M)$ . The luminosities of these satellite galaxies are drawn from the distribution  $\Phi_s(L|M)$ .

Phase space coordinates are assigned to the galaxies in the following manner. The central galaxy is assumed to reside at rest at the centre of the halo. Therefore, it has the same phase space coordinates as the parent dark matter halo. We assume that the halo is spherical and that the dark matter density distribution,  $\rho(r|M)$ , follows a universal profile (Navarro, Frenk & White 1997) given by

$$\rho(r|M) \propto \left(\frac{r}{r_s}\right)^{-1} \left(1 + \frac{r}{r_s}\right)^{-2}. \quad (3)$$

Here,  $r_s$  denotes a scale radius which is specified in terms of the virial radius,  $r_{\text{vir}}$ , using the concentration parameter,  $c(M) = r_{\text{vir}}/r_s$ . We use the concentration-mass relation from Macciò et al. (2007) appropriately modified for our definition of the halo mass. The number density distribution of satellites,  $n_{\text{sat}}(r|M)$ , is given by

$$n_{\text{sat}}(r|M) \propto \left(\frac{r}{\mathcal{R}r_s}\right)^{-\gamma} \left(1 + \frac{r}{\mathcal{R}r_s}\right)^{\gamma-3}, \quad (4)$$

where  $\gamma$  represents the slope of the number density distribution of satellites, as  $r \rightarrow 0$  and  $\mathcal{R}$  is a free parameter. For populating the MGC, we adopt  $\gamma = \mathcal{R} = 1$  which implies that the satellites trace the dark matter density distribution in an unbiased manner. The distribution,  $n_{\text{sat}}(r|M)$ , is normalized such that

$$\langle N_{\text{sat}} \rangle(M) = 4\pi \int_0^{r_{\text{vir}}} n_{\text{sat}}(r|M) r^2 dr. \quad (5)$$

The radial coordinates of the satellite galaxies with respect to the center of the halo are sampled from the distribution  $n_{\text{sat}}(r|M)$ . The satellite distribution around centrals is assumed to be spherically symmetric and random angular coordinates are assigned to the satellite galaxies. At the assigned position for every satellite galaxy, one dimensional velocities are drawn from a Gaussian,

$$f(v_j) = \frac{1}{\sqrt{2\pi}\sigma_{\text{sat}}(r|M)} \exp\left[-\frac{v_j^2}{2\sigma_{\text{sat}}^2(r|M)}\right], \quad (6)$$

where  $v_j$  denotes the relative velocity of the satellite with respect to the central along axis  $j$  and  $\sigma_{\text{sat}}^2(r|M)$  denotes the radial velocity dispersion at a distance  $r$  from the centre of the halo. Here isotropy of orbits is assumed, i.e. the velocity dispersion along the  $j^{\text{th}}$  axis,  $\sigma_j^2$ , equals  $\sigma_{\text{sat}}^2(r|M)$ . The radial velocity dispersion within the halo is determined by solving the Jeans equation

$$\sigma_{\text{sat}}^2(r|M) = \frac{1}{n_{\text{sat}}(r|M)} \int_r^{\infty} n_{\text{sat}}(r'|M) \frac{\partial\Psi}{\partial r'}(r'|M) dr', \quad (7)$$

where  $\Psi(r'|M)$  is the gravitational potential and the radial derivative represents the radial force given by

$$\frac{\partial\Psi}{\partial r}(r|M) = \frac{4\pi G}{r^2} \int_0^r \rho(r'|M) r'^2 dr'. \quad (8)$$

We assume that the dark matter dominates the potential. Using Eqs. (3) and (4) in Eqs. (7) and (8) gives

$$\sigma_{\text{sat}}^2(r|M) = \frac{c V_{\text{vir}}^2}{\mathcal{R}^2 \mu(c)} \left(\frac{r}{\mathcal{R}r_s}\right)^\gamma \left(1 + \frac{r}{\mathcal{R}r_s}\right)^{3-\gamma} \int_{r/r_s}^{\infty} \frac{\mu(x) dx}{(x/\mathcal{R})^{\gamma+2} (1+x/\mathcal{R})^{3-\gamma}}, \quad (9)$$

where  $V_{\text{vir}}$  is the circular velocity at  $r_{\text{vir}}$  and

$$\mu(x) = \int_0^x y(1+y)^{-2} dy. \quad (10)$$

The above expression for  $\sigma_{\text{sat}}^2(r|M)$  is used in the distribution given by Eq. (6) to assign velocities to satellites. The entire procedure of assigning central and satellite galaxies is repeated for all the dark matter haloes within the simulation.

Our aim is to construct a mock redshift survey that mimics the SDSS. Therefore, 2x2x2 identical galaxy-populated simulation boxes (which have periodic boundary conditions) are stacked together. A (RA,DEC) coordinate frame is defined with respect to a virtual observer at one of the corners of the stack. The apparent magnitude of each galaxy is computed according to its luminosity and distance from the observer. The line-of-sight (los) velocity of the galaxy is calculated by adding its peculiar velocity to the velocity of the cosmological flow. A random velocity drawn from a Gaussian distribution with a dispersion of  $35 \text{ km s}^{-1}$  is further added along the los to account for the spectroscopic redshift errors present in the SDSS. The redshift as seen by the virtual observer is then computed using the total velocity. We only consider galaxies with an observed redshift  $z < 0.15$  and an apparent magnitude brighter than 17.77. This flux limited catalogue is denoted henceforth by MOCKF and has 289,500 galaxies above an absolute luminosity of  $10^9 h^{-2} L_\odot$ . MOCKF is used in Appendix A to investigate potential selection biases associated with the selection of central galaxies. In addition to MOCKF, we construct a volume limited sample, MOCKV, of galaxies that lie in the redshift range  $0.02 \leq z \leq 0.072$  and have luminosities greater than  $10^{9.5} h^{-2} L_\odot$ . It consists of 69,512 galaxies. In what follows, we use the volume limited sample MOCKV to validate our method for quantifying the kinematics (Section 4), to validate the method to infer the number density distribution of satellites (Section 5) and finally to confirm

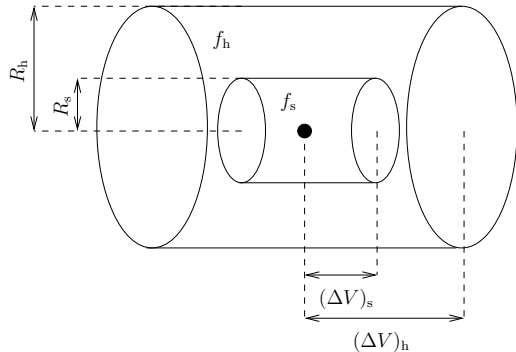


**Figure 1.** Schematic diagram of a selection criterion. Two coaxial cylinders are defined around each galaxy (represented by a solid dot). The axis is along the los while the face of each cylinder is parallel to the plane of the sky.

that the mean and scatter of the MLR can be reliably recovered using the kinematics of satellites (Section 6).

### 3 SELECTION CRITERIA

Large scale galaxy redshift surveys such as the SDSS allow the selection of a statistically significant sample of satellites. Since the observed galaxies cannot be *a priori* classified as centrals and satellites, it is important to use a selection criterion that can correctly identify central galaxies and the satellites which orbit around them. In this section, we describe the selection criterion that we use to identify the central and satellite galaxies.

A galaxy is identified to be a central if it is at least  $f_h$  times brighter than every other galaxy within a cylindrical volume specified by  $R < R_h$  and  $|\Delta V| < (\Delta V)_h$  (see Fig. 1). Here,  $R$  is the physical separation from the candidate central galaxy projected on the sky and  $\Delta V$  is the los velocity difference. Around each of the identified centrals, satellites are those galaxies that are at least  $f_s$  times fainter than their central galaxy and lie within a cylindrical volume specified by  $R < R_s$  and  $|\Delta V| < (\Delta V)_s$ . The identification of the central galaxies depends on the parameters  $R_h$ ,  $(\Delta V)_h$  and  $f_h$ , while the selection of satellites depends on the parameters  $R_s$ ,  $(\Delta V)_s$  and  $f_s$ . The values of these parameters also determine the level of contamination of the sample due to falsely identified centrals and falsely identified satellites (hereafter interlopers). The false identification of centrals can be minimized by choosing large values of  $R_h$ ,  $(\Delta V)_h$  and  $f_h$  so that the selected central is the dominant galaxy in a large volume. On the other hand, minimizing the interlopers requires small values of  $R_s$  and  $(\Delta V)_s$ . A large value of  $f_s$  further guarantees that the selected satellites are small and do not dominate the kinematics of the halo (i.e. can safely be considered as test particles). Although stricter restrictions yield cleaner samples, they also reduce the sample size significantly. This makes the velocity dispersion measurements noisy. Thus, there is a tradeoff between the contamination level and the sample size.

Most authors have chosen fixed values for the selection criterion parameters, independent of the luminosity of the galaxy under consideration (McKay et al. 2002; Prada et al. 2003; Brainerd & Specian 2003; N08). Since

**Table 1.** Selection Criteria

SC	$R_h$ Mpc/h	$(\Delta V)_h$ km/s	$f_h$	$R_s$ Mpc/h	$(\Delta V)_s$ km/s	$f_s$
ITER	2.0	4000	1.0	0.5	4000	1.0
	$0.8\sigma_{200}$	$1000\sigma_{200}$	1.0	$0.15\sigma_{200}$	4000	1.0
N08	1.0	2400	2.0	0.4	1200	8.0

The parameters used to specify the inner and the outer cylinder around a galaxy for the selection criterion used in this paper (ITER) and the one used in N08. The first row for ITER denotes the parameters used in the first iteration, while the second row denotes the parameters used in subsequent iterations. The velocity dispersion,  $\sigma_{\text{sat}}$  in units of  $200 \text{ km s}^{-1}$  is denoted by  $\sigma_{200}$  and is used to scale the cylinders in every iteration.

brighter centrals on average reside in more extended haloes, van den Bosch et al. (2004) advocated an aperture which scales with the virial radius of the halo around the galaxy. They used an iterative criterion which scales the cylindrical aperture based upon the estimate of the velocity dispersion around the central after every iteration. In this paper, we also use this iterative criterion to select centrals and satellites. The parameter set  $\{R_h, (\Delta V)_h, f_h, R_s, (\Delta V)_s, f_s\}$  that defines the inner and outer cylinders for the iterative criterion (ITER) is listed in Table 1. The first row lists the parameters for the first iteration while the next row lists the scaling of these parameters in the subsequent iterations. In short, we proceed as follows:

- (i) Use fixed values of the aperture size to select centrals and satellites in the first iteration.
- (ii) Fit the velocity dispersion of the selected satellites as a function of the central galaxy luminosity,  $\sigma_{\text{sat}}(L_c)$ , with a simple functional form (see Section 4.1).
- (iii) Select new centrals and satellites by scaling the inner and the outer cylinders based on the estimate of the velocity dispersion.
- (iv) Repeat (ii) and (iii) until  $\sigma_{\text{sat}}(L_c)$  has converged to the required accuracy.

For step (iii), we adopt the aperture scalings used in van den Bosch et al. (2004). These aperture scalings were optimised to yield a large number of centrals and satellites, but at the same time reduce the interloper contamination. The values chosen for  $R_h$  and  $R_s$  approximately correspond to 2 and 0.375 times the virial radius,  $r_{\text{vir}}$ .

### 4 SATELLITE KINEMATICS

In this section, we describe how to measure and model the velocity dispersion-luminosity relation,  $\sigma_{\text{sat}}(L_c)$ , using the satellites identified by the selection criterion. The relation  $\sigma_{\text{sat}}(L_c)$  can be measured either by binning the satellites by central galaxy luminosity or by using an unbinned estimator. We use the unbinned estimate after every iteration of the selection criterion to scale the selection aperture. However, to quantify the kinematics of the final sample of satellites, we use the binned estimator, for reasons which we describe further in the text. In the following subsections, we describe

**Table 2.** Parameters for the Selection Criterion

Sample	a	b	c
MOCKV	2.06	0.45	0.25
MOCKF	2.05	0.50	0.23
SDSSV	2.20	0.38	0.33

The parameters used in Eq. (11) to define  $\sigma_{200}$  as a function of the luminosity of a galaxy in the final iteration for samples MOCKV, MOCKF and for the volume-limited sample from the SDSS, denoted by SDSSV.

the unbinned and the binned estimators for  $\sigma_{\text{sat}}(L_c)$  and finally an analytical model for the same.

#### 4.1 Unbinned Estimates

We use a maximum likelihood method to estimate the relation  $\sigma_{\text{sat}}(L_c)$  from the velocity information of the selected satellites after every iteration of the selection criterion. Let  $\sigma_{200}$  denote  $\sigma_{\text{sat}}(L_c)$  in units of  $200 \text{ km s}^{-1}$  and  $L_{10}$  denote the luminosity of the central galaxy in units of  $10^{10} h^{-2} L_\odot$ . Following van den Bosch et al. (2004), we parametrize  $\sigma_{200}$  as,

$$\sigma_{200}(\log L_{10}) = a + b (\log L_{10}) + c (\log L_{10})^2. \quad (11)$$

Let  $f_{\text{int}}$  denote the interloper fraction and assume that this fraction is independent of the luminosity of the central galaxy and  $\Delta V$ . The probability for a selected satellite to have a los velocity difference of  $\Delta V \text{ km s}^{-1}$  with respect to the central is then given by

$$P(\Delta V) = \frac{f_{\text{int}}}{2(\Delta V)_s} + \frac{1 - f_{\text{int}}}{\bar{\omega}} \exp \left[ -\frac{(\Delta V)^2}{2\sigma_{\text{eff}}^2} \right], \quad (12)$$

where,  $\sigma_{\text{eff}} = [\sigma_{\text{sat}}^2 + \sigma_{\text{err}}^2]^{1/2}$  is the effective velocity dispersion in the presence of the redshift errors and the factor

$$\bar{\omega} = \sqrt{2\pi} \sigma_{\text{eff}} \text{erf} \left[ \frac{(\Delta V)_s}{\sqrt{2}\sigma_{\text{eff}}} \right], \quad (13)$$

is such that the  $P(\Delta V)$  is properly normalized to unity. In our attempt to mimic SDSS, we have added a Gaussian error of  $35 \text{ km s}^{-1}$  to the velocity of each galaxy in the mock catalog. Therefore, the error on the velocity difference,  $\Delta V$ , of the central and satellite galaxies is  $\sigma_{\text{err}} = \sqrt{2} \times 35 \text{ km s}^{-1}$  which adds in quadrature to  $\sigma_{\text{sat}}$  to yield  $\sigma_{\text{eff}}$ .

We use Powell's direction set method to determine the parameters ( $a$ ,  $b$ ,  $c$ ,  $f_{\text{int}}$ ) that maximize the likelihood  $\mathcal{L} = \sum_i \ln[P(\Delta V)]_i$ , where the summation is over all the selected satellites. This yields a continuous estimate of  $\sigma_{\text{sat}}(L_c)$  without the need to bin the los velocity information of satellites according to the luminosity of the central galaxy. The parameter set ( $a$ ,  $b$ ,  $c$ ) fitted in the last but one iteration determines the size of the apertures used to select the final sample of satellites. The values of these parameters for the samples investigated in this paper are listed in Table 2.

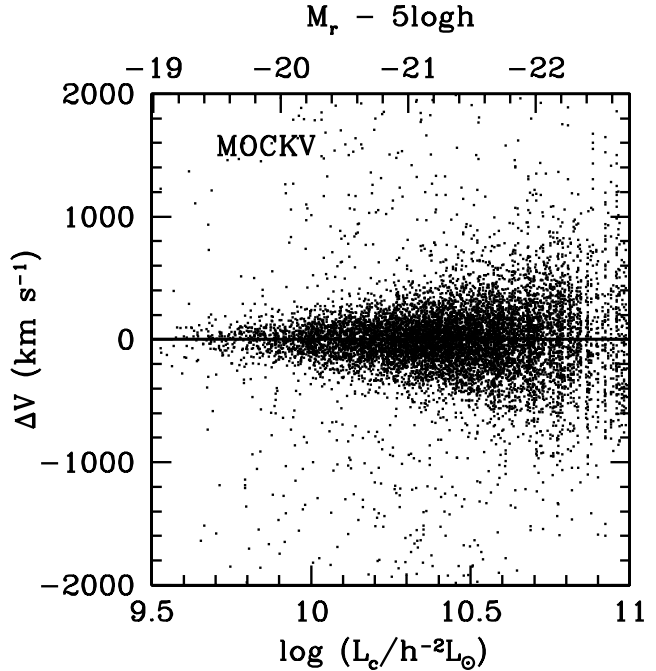


**Figure 2.** Scatter plot of the velocity difference,  $\Delta V$ , between the satellites and their centrals as a function of the central galaxy luminosity. The satellites were obtained by applying the iterative selection criterion to MOCKV.

#### 4.2 Binned Estimates

We use a binned estimator to quantify the kinematics of the final sample of satellites. The binned estimator allows us to relax the simplistic assumption of  $f_{\text{int}}$  being independent of  $L_c$ . More importantly, the binned estimator allows us, in a straightforward manner, to measure  $\sigma_{\text{sat}}(L_c)$  using two different weighting schemes - satellite-weighting and host-weighting. Most studies in the literature have used one of these two weighting schemes to infer the mean of the MLR. However, as demonstrated in Paper I, the mean of the MLR inferred from the velocity dispersion in any one of these two schemes is degenerate with the scatter in the MLR. This degeneracy can be broken by modelling the velocity dispersions in both schemes *simultaneously*. In what follows, we briefly explain these two weighting schemes in turn and then verify that the velocity dispersions in both schemes can be accurately recovered from the MGC.

To measure the velocity dispersion of satellites in the satellite-weighting scheme, we obtain the distribution of velocities of the satellites,  $P(\Delta V)$ , with respect to their centrals for several bins of central galaxy luminosity (see Fig. 3). Each bin has a width  $\Delta \log[L_c] = 0.15$ . In this scheme, the centrals that have a larger number of satellites clearly contribute more to the  $P(\Delta V)$  distribution than those which have a smaller number of satellites. Therefore, the resulting scatter in  $P(\Delta V)$  is a satellite-weighted average of the velocity dispersions around the stacked centrals (see Paper I for a detailed discussion). The dispersion obtained using this scheme is denoted henceforth by  $\sigma_{\text{sw}}$ .

One has to undo the satellite-weighting described above in order to measure the host-weighted velocity dispersion. This can be accomplished by introducing a weight  $w = N^{-1}$  for each central-satellite pair while constructing the  $P(\Delta V)$

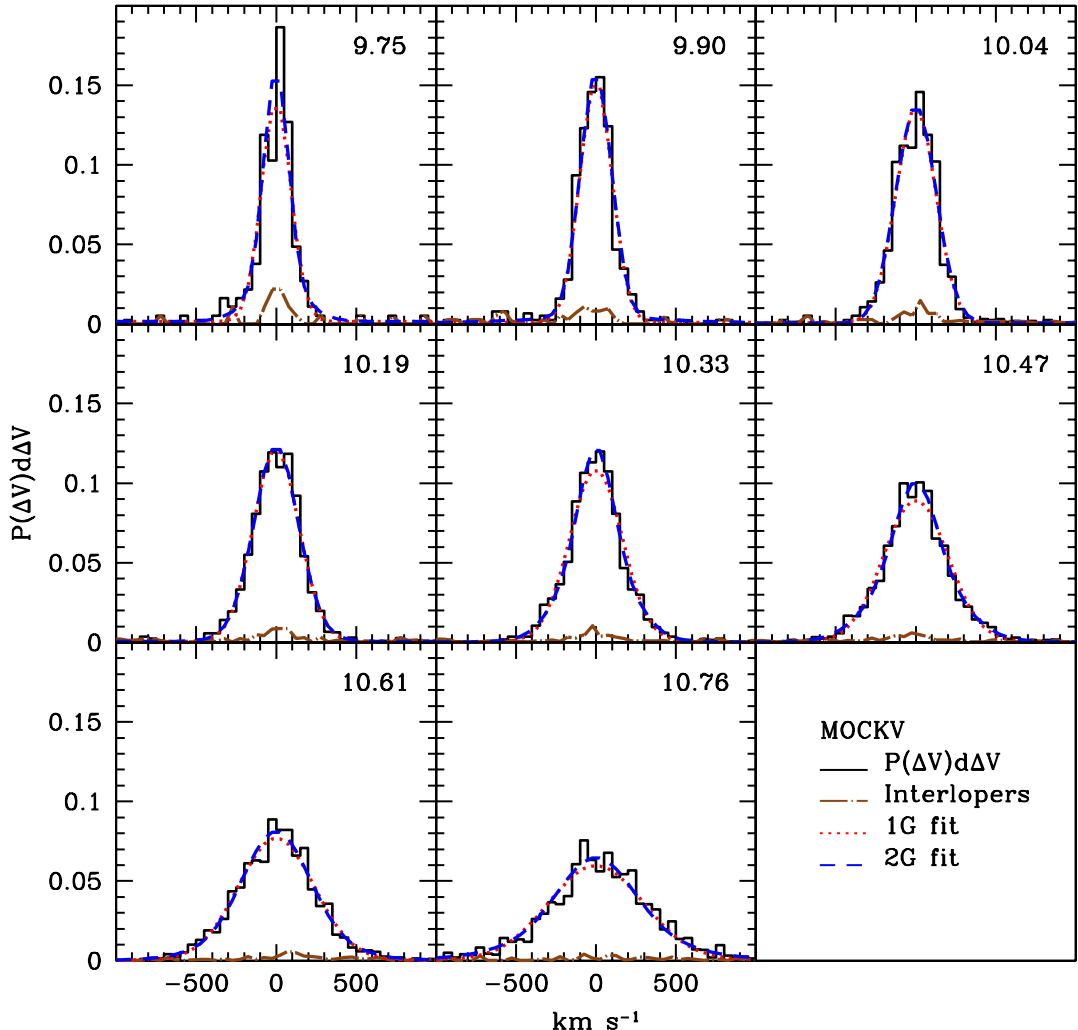


**Figure 3.** The satellite-weighted  $P(\Delta V)$  distributions of satellites around centrals selected in several luminosity bins from MOCKV. The average  $\log(L_c/h^{-2}L_\odot)$  for each bin is indicated at the upper right corner of every panel. The (brown) dot-dashed line at the bottom of each distribution shows the contamination of the  $P(\Delta V)$  distributions due to the interlopers. The (red) dotted lines indicate the single Gaussian fits, the (blue) dashed lines the double Gaussian fits.

distribution (van den Bosch et al. 2004; Conroy et al. 2007; Becker et al. 2007). Here,  $N$  denotes the number of satellites selected around the central under consideration. Therefore, in this scheme each central receives a total weight of unity irrespective of the number of satellites it hosts. The scatter in this weighted  $P(\Delta V)$  distribution is the host-weighted velocity dispersion and is denoted henceforth by  $\sigma_{\text{hw}}$ .

The procedure to obtain the scatter in the  $P(\Delta V)$  distributions is the same for both the satellite-weighted and the host-weighted case. This procedure must account for the interlopers and the redshift errors present in MOCKV. In what follows, we illustrate this procedure only for the satellite-weighted case.

Fig. 2 shows the scatter plot of velocity difference  $\Delta V$  of the selected satellites and the centrals as a function of the luminosity of the centrals. The satellite-weighted  $P(\Delta V)$  distributions of the satellites selected from MOCKV for several central luminosity bins are shown in Fig. 3. Dot-dashed lines show the contamination of the  $P(\Delta V)$  distributions due to interlopers and are barely visible at the bottom of each dis-

tribution. This confirms the claims in van den Bosch et al. (2004) that the iterative criterion yields a small fraction of interlopers with a weak dependence on  $L_c$  and that the interlopers can be modelled as a constant contribution to the velocity distribution independent of  $\Delta V$ .

A simple way to estimate the scatter of a  $P(\Delta V)$  distribution is to fit a Gaussian plus a constant model given by

$$P(\Delta V) = a_0 + a_1 \exp \left[ \frac{-(\Delta V)^2}{2\sigma_{\text{eff}}^2} \right]. \quad (14)$$

Here,  $a_0$  denotes the constant (with respect to  $\Delta V$ ) interloper background,  $a_1$  is the normalization of the Gaussian and  $\sigma_{\text{eff}}$  is the effective dispersion in the presence of the redshift errors.

The velocity dispersion obtained using a single Gaussian plus constant model fit can be systematically affected if the  $P(\Delta V)$  distribution is intrinsically non-Gaussian. Diaferio & Geller (1996) demonstrated that the velocity distribution can be non-Gaussian partly due to mass mixing

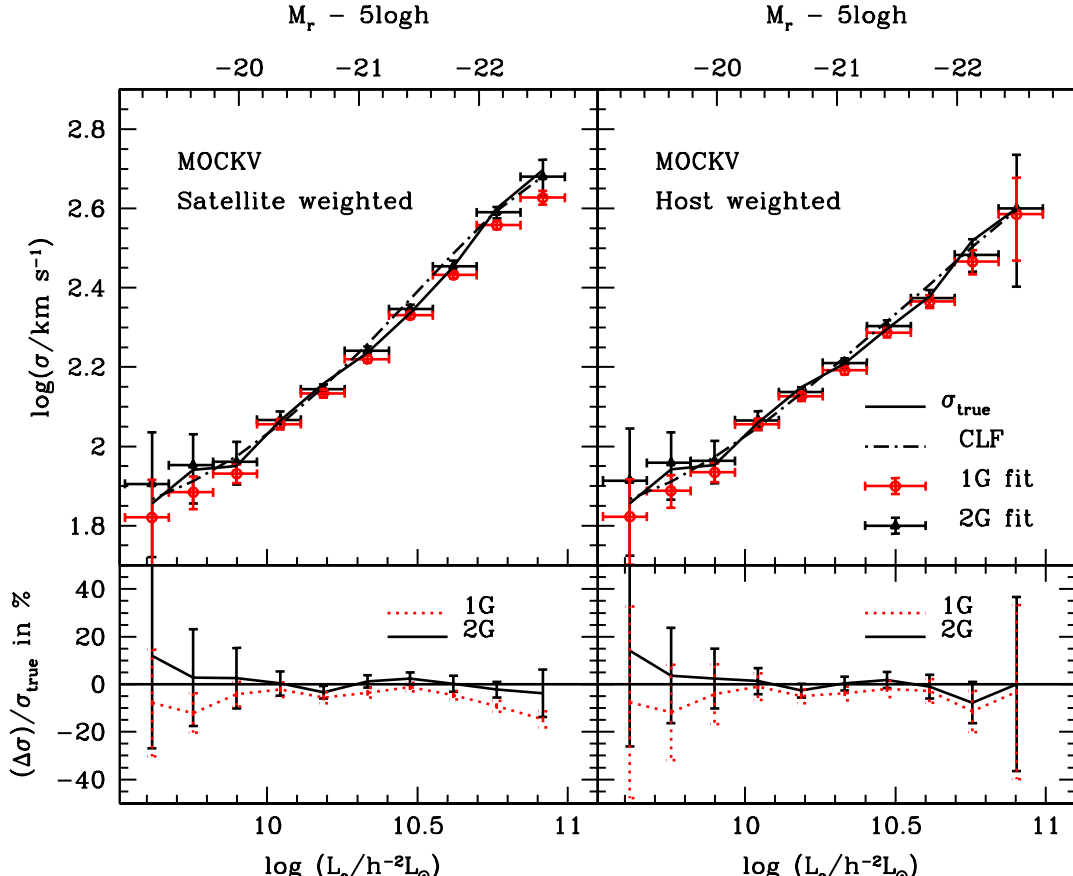


**Figure 4.** Upper panels show the satellite-weighted and the host-weighted velocity dispersions recovered from MOCKV. The (red) circles show values recovered from a single Gaussian fit while the (black) triangles show those from the double Gaussian fit. The solid line shows the variance of the true satellites and the dot-dashed line shows the analytical prediction using the halo occupation statistics of centrals from the MGC. The bottom panel plots the percentage deviation of the single and double Gaussian fits from the variance of the true satellites.

(which is the result of stacking haloes of different mass) and partly due to the unrelaxed state of a halo. The second moment of such a non-Gaussian distribution can be estimated with a double Gaussian plus a constant model (Becker et al. 2007) given by

$$P(\Delta V) = a_0 + a_1 \exp \left[ \frac{-(\Delta V)^2}{2\sigma_1^2} \right] + a_2 \exp \left[ \frac{-(\Delta V)^2}{2\sigma_2^2} \right]. \quad (15)$$

The scatter,  $\sigma_{\text{eff}}$ , in this case is such that

$$\sigma_{\text{eff}}^2 = \frac{a_1 \sigma_1^3 + a_2 \sigma_2^3}{a_1 \sigma_1 + a_2 \sigma_2} = \sigma_{\text{sw}}^2 + \sigma_{\text{err}}^2. \quad (16)$$

The dotted and the dashed lines in Fig. 3 show the single and double Gaussian fits to the  $P(\Delta V)$  distributions respectively.

Fig. 4 shows the velocity dispersions obtained from the satellite-weighted  $P(\Delta V)$  distributions in the upper left panel and those obtained from the host-weighted  $P(\Delta V)$  distributions in the upper right panel. The (red) circles and the (black) triangles indicate the single and the double Gaussian fits respectively. Since the true satellites of centrals selected from MOCKV are known, they can be used to judge the goodness of the fits. The satellite-weighted and the host-weighted velocity dispersions of the true satellites (among

the satellites selected using the iterative criterion) are obtained using

$$\sigma_{\text{true}}^2 = \frac{\sum_{j=1}^{N_c} \sum_{i=1}^{N_j} w_{ij} (\Delta V)_{ij}^2}{\sum_{j=1}^{N_c} \sum_{i=1}^{N_j} w_{ij}} - \sigma_{\text{err}}^2. \quad (17)$$

Here,  $N_c$  denotes the number of true centrals,  $N_j$  denotes the number of true satellites of the  $j^{\text{th}}$  central and  $(\Delta V)_{ij}$  denotes the los velocity difference of the  $j^{\text{th}}$  central with respect to its  $i^{\text{th}}$  satellite. The weight  $w_{ij} = 1$  for the satellite-weighted case and  $w_{ij} = N_j^{-1}$  for the host-weighted case. The true velocity dispersions thus obtained are shown as solid curves in Fig. 4.

The bottom panels of Fig. 4 show the percentage deviation of both the single and the double Gaussian fits from the velocity dispersions of the true satellites. The single Gaussian fit (the dotted line) underestimates the dispersions systematically by about 5 – 10%. The double Gaussian fit (the solid line) on the other hand gives an unbiased estimate of both velocity dispersions. Therefore, in what follows, we use the double Gaussian fit for measuring both the satellite-weighted and the host-weighted velocity dispersions (cf. Becker et al. 2007).

### 4.3 Analytical Estimates

We now compare the velocity dispersions obtained from the satellite-weighted and the host-weighted schemes to their analytical expectation values. As detailed in Paper I, the satellite-weighted and the host-weighted velocity dispersions depend on the distribution of halo masses of central galaxies specified by  $P(M|L_c)$ . The analytical expressions describing the velocity dispersion in these two weighting schemes are

$$\sigma_{\text{sw}}^2(L_c) = \frac{\int_0^\infty P(M|L_c) \langle N_{\text{sat}} \rangle_{\text{ap},M} \langle \sigma_{\text{sat}}^2 \rangle_{\text{ap},M} dM}{\int_0^\infty P(M|L_c) \langle N_{\text{sat}} \rangle_{\text{ap},M} dM}, \quad (18)$$

$$\sigma_{\text{hw}}^2(L_c) = \frac{\int_0^\infty P(M|L_c) \mathcal{P}(\langle N_{\text{sat}} \rangle_{\text{ap},M}) \langle \sigma_{\text{sat}}^2 \rangle_{\text{ap},M} dM}{\int_0^\infty P(M|L_c) \mathcal{P}(\langle N_{\text{sat}} \rangle_{\text{ap},M}) dM}. \quad (19)$$

Here, the average number of satellites and the average velocity dispersion of satellites, within the aperture  $R_s$  in a halo of mass  $M$ , are denoted by  $\langle N_{\text{sat}} \rangle_{\text{ap},M}$  and  $\langle \sigma_{\text{sat}}^2 \rangle_{\text{ap},M}$  respectively. The number of satellites within the aperture,  $\langle N_{\text{sat}} \rangle_{\text{ap},M}$ , is given by

$$\langle N_{\text{sat}} \rangle_{\text{ap},M} = 4\pi \int_0^{R_s} R dR \int_R^{r_{\text{vir}}} n_{\text{sat}}(r|M) \frac{r dr}{\sqrt{r^2 - R^2}}. \quad (20)$$

Assuming the velocity dispersion of satellites to be isotropic, the velocity dispersion,  $\langle \sigma_{\text{sat}}^2 \rangle_{\text{ap},M}$ , can be expressed as the average of the radial velocity dispersion,  $\sigma_{\text{sat}}^2(r|M)$  (see Eq. 9), over the aperture  $R_s$ ,

$$\langle \sigma_{\text{sat}}^2 \rangle_{\text{ap},M} = \frac{4\pi}{\langle N_{\text{sat}} \rangle_{\text{ap},M}} \int_0^{R_s} R dR \int_R^{r_{\text{vir}}} n_{\text{sat}}(r|M) \sigma_{\text{sat}}^2(r|M) \frac{r dr}{\sqrt{r^2 - R^2}}. \quad (21)$$

Note that, when measuring the host-weighted velocity dispersions only satellites of those centrals that have at least one satellite within the search aperture are used. The fraction of such centrals is denoted by  $\mathcal{P}(\langle N_{\text{sat}} \rangle_{\text{ap},M})$  and is given by the probability that a halo of mass  $M$ , which on average hosts  $\langle N_{\text{sat}} \rangle_{\text{ap},M}$  satellites within the aperture  $R_s$ , has  $N_{\text{sat}} \geq 1$  within the aperture. Therefore,

$$\begin{aligned} \mathcal{P}(\langle N_{\text{sat}} \rangle_{\text{ap},M}) &\equiv P(N_{\text{sat}} \geq 1) \\ &= 1 - P(N_{\text{sat}} = 0) \\ &= 1 - \exp[-\langle N_{\text{sat}} \rangle_{\text{ap},M}] \end{aligned} \quad (22)$$

In the last equality we have assumed that the satellite occupation numbers (cf. Eq. 2) follow Poisson statistics, which is supported by numerical simulations (Kravtsov et al. 2004) and by results from group catalogs based on SDSS (Yang et al. 2005a; Yang, Mo & van den Bosch 2008). The factor  $\mathcal{P}(\langle N_{\text{sat}} \rangle_{\text{ap},M})$  is not considered in the analytical estimate in the satellite-weighting scheme as haloes with zero satellites, by definition, contribute zero weight.

From the above analytical description, it is clear that the analytical estimates for the velocity dispersions require the knowledge of

- the density distribution of dark matter haloes,  $\rho(r|M)$
- the number density distribution of satellites,  $n_{\text{sat}}(r|M)$
- the halo occupation statistics of centrals,  $P(M|L_c)$ , and the halo occupation number of satellites,  $\langle N_{\text{sat}} \rangle(M)$ .

We assume that the density distribution of dark matter haloes is given by Eq. (3) and that the number density

distribution of satellites is given by Eq. (4) with  $\gamma = \mathcal{R} = 1$ . The halo occupation statistics of centrals,  $P(M|L_c)$  is given by

$$P(M|L_c) = \frac{\Phi_c(L_c|M)n(M)}{\int \Phi_c(L_c|M)n(M)dM} \quad (23)$$

where  $\Phi_c(L_c|M)$  is the conditional luminosity function of central galaxies and  $n(M)$  is the halo mass function. The number of satellite galaxies in a halo of mass  $M$  is given by Eq. (1). We adopt the  $\Phi_c(L_c|M)$  and  $\Phi_s(L|M)$  that were used in Section 2 to populate the MGC. With this input, we compute the analytical estimates for the velocity dispersions of satellites as a function of luminosity using Eqs. (18) and (19). The results thus obtained are shown as dot-dashed curves in the corresponding panels of Fig. 4. Overall the agreement with the velocity dispersions obtained from the satellites in the MGC is very good, except at intermediate luminosities where the analytical estimates are  $\sim 5$  percent higher than  $\sigma_{\text{true}}$ . This indicates that the central galaxies selected from the MGC do not properly sample the full  $P(M|L_c)$ . This can have two reasons: (i) a systematic problem with the criterion used to select central galaxies, or (ii) cosmic variance due to the finite volume probed by MOCKV. As we demonstrate in Appendix A our iterative criterion accurately samples the true  $P(M|L_c)$ , except for the fact that it misses the haloes of those centrals which have zero satellites. However, this sampling effect is accounted for in our analytical model via Eq. (22). In fact detailed tests show that the discrepancies between  $\sigma_{\text{true}}$  and our analytical estimates are entirely due to cosmic variance in the MGC.

In Appendix A, we also show that the strict selection criteria, that have been abundantly used in the literature, lead to a sample of central galaxies that is biased to reside in relatively low mass haloes. Consequently, the resulting MLR of central galaxies is similarly biased, and has to be interpreted with great care.

### 5 NUMBER DENSITY DISTRIBUTION OF SATELLITES

As described above, the number density distribution of satellite galaxies,  $n_{\text{sat}}(r|M)$ , is a necessary input to analytically compute the velocity dispersions. The projected number density distribution of satellites,  $\Sigma(R|L_c)$ , around centrals of a given luminosity, directly reflects the functional form of  $n_{\text{sat}}(r|M)$ . The distribution  $\Sigma(R|L_c)$  can be directly measured by combining the satellites around centrals of a given luminosity,  $L_c$ , chosen by the selection criterion. However, it is necessary to first assess the impact of the interloper contamination on the measurement of  $\Sigma(R|L_c)$ , for which we again make use of the satellite sample selected from MOCKV.

Fig. 5 shows, for the five brightest luminosity bins, the azimuthally averaged projected number density distributions of the satellites selected from MOCKV. The errorbars reflect the Poisson noise on the number of satellites in each radial bin. The abrupt cutoff at large  $R$  is an artefact due to the parameter  $R_s$  in the selection criterion which describes the maximum projected radius within which satellites get selected. Note that, since  $R_s$  depends upon the luminosity

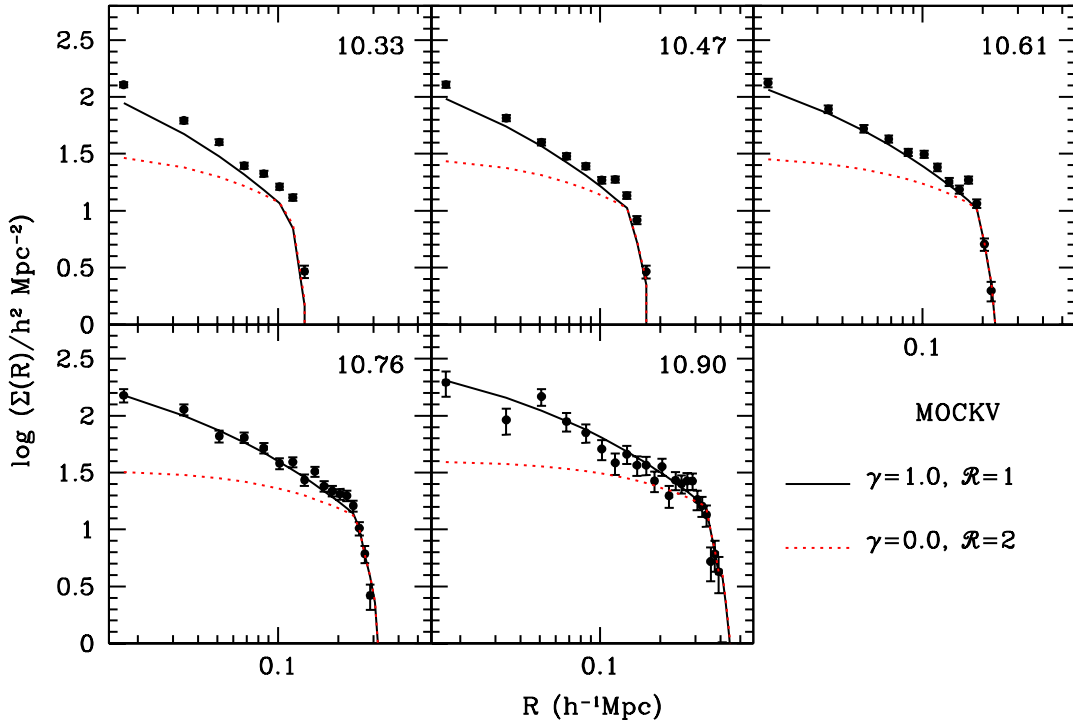


**Figure 5.** The projected number density distributions of the satellites selected from MOCKV as a function of the projected radius in the brightest central luminosity bins. The errorbars assume Poisson statistics for the number of satellites in each bin. The (black) solid lines indicate the analytical predictions and assume that the satellite number density distribution follows the dark matter distribution in an unbiased manner, i.e.  $\mathcal{R} = 1$  and  $\gamma = 1$  in eq. (4). For comparison, the (red) dotted lines show the analytical predictions that assume  $\mathcal{R} = 2$  and  $\gamma = 0$ .

of central galaxies under consideration, this cutoff shifts to larger  $R$  with increasing central galaxy luminosity.

The projected number density distribution of satellites around centrals stacked according to luminosity,  $\Sigma(R|L_c)$ , can be analytically expressed as,

$$\Sigma(R|L_c) = \frac{\int P(M|L_c) \Sigma(R|M) dM}{\int P(M|L_c) \mathcal{P}(\langle N_{\text{sat}} \rangle_{\text{ap},M}) dM}. \quad (24)$$

Here,  $\Sigma(R|M)$  is the projection of  $n_{\text{sat}}(r|M)$  along the line-of-sight and is given by

$$\Sigma(R|M) = \int_R^{r_{\text{vir}}} \frac{n_{\text{sat}}(r|M) 2r dr}{\sqrt{r^2 - R^2}}, \quad (25)$$

Using  $n_{\text{sat}}(r|M)$  given by Eq. (4) with  $\mathcal{R} = \gamma = 1$  and the true  $P(M|L_c)$  present in the MGC, we analytically compute the expected number density distribution of satellites around centrals of a given luminosity. The solid lines in Fig. 5 show the results of this analytical expectation. The small differences between the measured and the analytically obtained distributions are due to the interlopers in the sample. However, the differences become negligible in the brighter luminosity bins. For comparison, the (red) dotted lines show the expected  $\Sigma(R|L_c)$  for  $\mathcal{R} = 2$  and  $\gamma = 0$ . This shows that the parameters  $\mathcal{R}$  and  $\gamma$ , that characterize the number density distribution of satellites, can be inferred from the projected number density distributions of the selected satellites.

## 6 MASS-LUMINOSITY RELATIONSHIP

In the previous sections, using a mock catalog, we have demonstrated that the satellite-weighted velocity dispersions, the host-weighted velocity dispersions and the projected number density distributions of satellites around centrals of a given luminosity can be reliably measured starting from a volume limited redshift catalog of galaxies. Next, we attempt to infer the MLR of central galaxies from the velocity dispersions measured from MOCKV. The aim is to invert Eqs. (18) and (19) which describe the dependence of the velocity dispersions on the MLR of central galaxies. In addition to the velocity dispersions, we also measure the average number of satellites per central of a given luminosity,  $\langle N_{\text{sat}} \rangle(L_c)$ , and use this as a constraint. The dependence of  $\langle N_{\text{sat}} \rangle(L_c)$  on the MLR of central galaxies is given by

$$\langle N_{\text{sat}} \rangle(L_c) = \frac{\int_0^{\infty} P(M|L_c) \langle N_{\text{sat}} \rangle_{\text{ap},M} dM}{\int_0^{\infty} P(M|L_c) \mathcal{P}(\langle N_{\text{sat}} \rangle_{\text{ap},M}) dM}. \quad (26)$$

In this section, we first describe the model we use to infer the mean and the scatter of the MLR from the observables  $\sigma_{\text{sw}}$ ,  $\sigma_{\text{hw}}$  and  $\langle N_{\text{sat}} \rangle$ . Next, we use this model to infer the mean and the scatter of the MLR in the MGC and compare it to the true relations present in the MGC.

### 6.1 The Model

As mentioned earlier, the analytical computation of  $\sigma_{\text{sw}}$ ,  $\sigma_{\text{hw}}$  and  $\langle N_{\text{sat}} \rangle$  requires the knowledge of the density distribution of dark matter haloes, the number density distribution

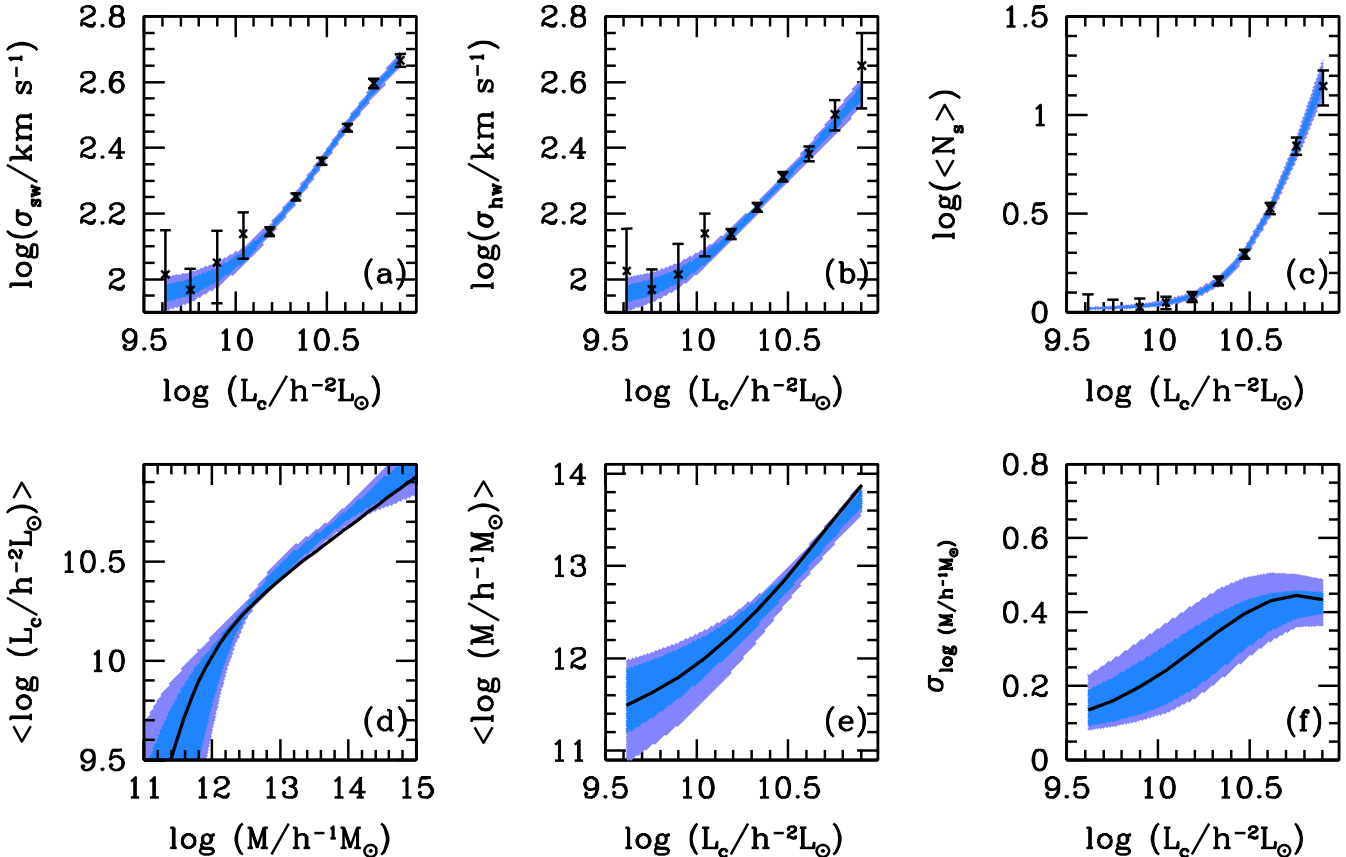


**Figure 6.** Crosses with errorbars in the upper panels denote the data used to constrain the Monte Carlo Markov Chain; the satellite-weighted velocity dispersions in panel (a), the host-weighted velocity dispersions in panel (b) and the average number of satellites per central in panel (c). The relations recovered from the MCMC analysis are shown in the bottom panels;  $\langle \log L_c \rangle(M)$  in panel (d),  $\langle \log M \rangle(L_c)$  in panel (e) and  $\sigma_{\log M}(L_c)$  in panel (f). In each panel, the blue and purple colours denote the 68% and the 95% confidence levels. The solid lines in the lower panels denote the true relations present in MOCKV.

**Table 3.** MOCKV: Parameters recovered from the MCMC

Parameter	Input	16%	50%	84%
$\log(L_0)$	9.93	9.64	10.01	10.32
$\log(M_1)$	11.04	10.48	11.28	11.69
$\gamma_2$	0.25	0.18	0.26	0.32
$\sigma_{\log L}$	0.14	0.13	0.15	0.17

The input parameters that describe  $P(L_c|M)$  are compared to the 16<sup>th</sup>, 50<sup>th</sup> and the 84<sup>th</sup> percentiles of the corresponding distributions of parameters obtained from the MCMC.

of satellites and the halo occupation statistics of centrals and satellites. We assume that the density distribution of dark matter haloes follows the NFW profile given by Eq. (3). For the number density distribution of satellites within a halo of mass  $M$ ,  $n_{\text{sat}}(r|M)$ , we use Eq. (4) with  $\mathcal{R} = \gamma = 1$ . As shown in Section 5, the projected number density distributions of satellites selected from MOCKV is consistent with this analytical expression. Next, we describe our model for the halo occupation statistics of the centrals, specified by  $P(M|L_c)$ , and the satellites, specified by  $\langle N_{\text{sat}} \rangle(M)$ .

The distribution  $P(M|L_c)$  is related to the complementary distribution,  $P(L_c|M)$ , by Bayes' theorem

$$P(M|L_c) = \frac{n(M)P(L_c|M)}{\int n(M)P(L_c|M)dM}, \quad (27)$$

where  $n(M)$  is the halo mass function. We follow Cacciato et al. (2008) and parametrize the distribution  $P(L_c|M)$  as a lognormal in  $L_c$ ,

$$P(L_c|M)dL_c = \frac{\log(e)}{\sqrt{2\pi}\sigma_{\log L}} \exp\left[-\frac{(\log[L_c/\tilde{L}_c])^2}{2\sigma_{\log L}^2}\right] \frac{dL_c}{L_c}. \quad (28)$$

Here  $\log \tilde{L}_c(M)$  denotes the mean of the lognormal distribution and  $\sigma_{\log L}$  is the scatter in this distribution. We use four parameters to specify the relation  $\tilde{L}_c(M)$ : a low mass end slope,  $\gamma_1$ , a high mass end slope,  $\gamma_2$ , a characteristic mass scale,  $M_1$ , and a normalisation,  $L_0$ ;

$$\tilde{L}_c = L_0 \frac{(M/M_1)^{\gamma_1}}{[1 + (M/M_1)]^{\gamma_1 - \gamma_2}}. \quad (29)$$

We assume the scatter  $\sigma_{\log L}$  to be independent of mass. We do not explore the faint end slope,  $\gamma_1$ , in our analysis as the velocity dispersions at the faint end are very uncertain due to low number statistics. Instead, we keep it fixed at 3.273, which is the value obtained from the analysis of the abundance and clustering of galaxies (see Cacciato et al. 2008). This parametrization is motivated by results of Yang, Mo & van den Bosch (2008) who measure

the conditional luminosity function from the SDSS group catalogue described in Yang et al. (2007).

We model the satellite occupation number,  $\langle N_{\text{sat}} \rangle(M)$ , as a power law distribution, given by

$$\langle N_{\text{sat}} \rangle(M) = N_s \left( \frac{M}{10^{12} h^{-1} M_{\odot}} \right)^{\alpha}, \quad (30)$$

which adds two more parameters ( $N_s, \alpha$ ). Thus, in total, our model has six free parameters ( $\sigma_{\log L}, L_0, M_1, \gamma_2, N_s, \alpha$ ). Given these parameters and the radial number density distribution of satellites (specified by  $\mathcal{R}$  and  $\gamma$ ), the velocity dispersions  $\sigma_{\text{sw}}(L_c)$  and  $\sigma_{\text{hw}}(L_c)$  as well as the number of satellites per central,  $\langle N_{\text{sat}} \rangle(L_c)$  in an aperture of a given size can be computed using Eqs. (18), (19) and (26) and compared to the measured values. Crosses with errorbars in Panels (a), (b) and (c) of Fig. 6 show  $\sigma_{\text{sw}}$ ,  $\sigma_{\text{hw}}$  and  $\langle N_{\text{sat}} \rangle$  as a function of the luminosity of the central obtained from MOCKV. We use these measurements to constrain the six free parameters of our model.

## 6.2 Monte-Carlo Markov Chain

To determine the posterior probability distributions of the 6 free parameters in our model, we use the Monte-Carlo Markov Chain (hereafter MCMC) technique. The MCMC is a chain of models, each with 6 parameters. At any point in the chain, a trial model is generated with the 6 free parameters drawn from 6 independent Gaussian distributions which are centred on the current values of the corresponding parameters. The chi-squared statistic,  $\chi^2_{\text{try}}$ , for this trial model, is calculated using

$$\chi^2_{\text{try}} = \chi^2_{\text{sw}} + \chi^2_{\text{hw}} + \chi^2_{\text{ns}}, \quad (31)$$

with

$$\chi^2_{\text{sw}} = \sum_{i=1}^{10} \left[ \frac{\sigma_{\text{sw}}(L_c[i]) - \hat{\sigma}_{\text{sw}}(L_c[i])}{\Delta \hat{\sigma}_{\text{sw}}(L_c[i])} \right]^2, \quad (32)$$

$$\chi^2_{\text{hw}} = \sum_{i=1}^{10} \left[ \frac{\sigma_{\text{hw}}(L_c[i]) - \hat{\sigma}_{\text{hw}}(L_c[i])}{\Delta \hat{\sigma}_{\text{hw}}(L_c[i])} \right]^2, \quad (33)$$

$$\chi^2_{\text{ns}} = \sum_{i=1}^{10} \left[ \frac{\langle N_{\text{sat}} \rangle(L_c[i]) - \hat{N}_{\text{sat}}(L_c[i])}{\Delta \hat{N}_{\text{sat}}(L_c[i])} \right]^2. \quad (34)$$

(35)

Here  $\hat{X}$  denotes the observational constraint  $X$  and  $\Delta \hat{X}$  its corresponding error. The trial step is accepted with a probability given by

$$P_{\text{accept}} = \begin{cases} 1.0, & \text{if } \chi^2_{\text{try}} \leq \chi^2_{\text{cur}} \\ \exp[-(\chi^2_{\text{try}} - \chi^2_{\text{cur}})/2], & \text{if } \chi^2_{\text{try}} > \chi^2_{\text{cur}} \end{cases} \quad (36)$$

where  $\chi^2_{\text{cur}}$  denotes the  $\chi^2$  for the current model in the chain.

We initialize the chain from a random position in the parameter space and discard the first  $10^4$  models allowing the chain to sample from a more probable part of the distribution. This is called the burn-in period for the chain. We proceed and construct a chain of models consisting of 10 million models. We thin this chain by a factor of  $10^4$  to remove the correlations between neighbouring models. This leaves us with a chain of 1000 independent models that sample the

posterior distribution. We use this chain of models to estimate the confidence levels on the parameters and relations of interest.

In Table 3, we compare the 16<sup>th</sup>, 50<sup>th</sup> and the 84<sup>th</sup> percentiles of the distributions of parameters, which characterize  $P(L_c|M)$ , obtained from the MCMC with the corresponding true values of these parameters present in MOCKV. The true parameter values have been recovered within the 68% confidence intervals. The 68 and 95% confidence levels in panels (a), (b) and (c) of Fig. 6 show that the models from the MCMC accurately fit the velocity dispersions,  $\sigma_{\text{sw}}$  and  $\sigma_{\text{hw}}$ , as well as the average number of satellites per central,  $\langle N_{\text{sat}} \rangle$  as a function of central galaxy luminosity. The confidence levels for the average luminosity of the centrals as a function of the halo mass,  $\tilde{L}_c(M)$ , are shown in panel (d). The confidence levels on the mean,  $\langle \log M \rangle(L_c)$ , and the scatter,  $\sigma_{\log M}(L_c)$ , of the MLR of central galaxies are shown in panels (e) and (f) respectively. The solid lines in the lower panels show the corresponding true relations present in MOCKV. Clearly, our method is able to accurately recover the true MLR.

This completes our tests with the MGC. Employing a variety of tests on a realistic MGC, we have established a proof-of-concept that, starting from a redshift survey of galaxies, one can reliably select central and satellite galaxies, quantify the kinematics of the selected satellites around central galaxies and use this information to infer an unbiased estimate of the mean and the scatter of the MLR of central galaxies.

## 7 RESULTS FROM SLOAN DIGITAL SKY SURVEY ANALYSIS

We now apply the method tested in the previous sections to data from the Sloan Digital Sky Survey (SDSS; York et al. 2000) which is a joint five-passband ( $u, g, r, i$  and  $z$ ) imaging and medium resolution ( $R \sim 1800$ ) spectroscopic survey. More specifically, we use the New York University Value Added Galaxy Catalogue (Blanton et al. 2005), which is based upon SDSS Data Release 4 (Adelman-McCarthy et al. 2006) but includes a set of significant improvements over the original pipelines. From this catalog, we select all galaxies in the main galaxy sample with redshifts in the range  $0.02 \leq z \leq 0.072$  and with a redshift completeness limit  $C > 0.8$ . We construct a volume limited sample of galaxies that have a  $r$ -band luminosity (k-corrected to redshift 0.1) above  $L_{\text{min}} = 10^{9.5} h^{-2} L_{\odot}$ . This sample is henceforth denoted by SDSSV. It consists of 57,593 galaxies. The SDSSV data is analysed assuming the cosmological parameters from the 3 year data release of WMAP (Spergel et al. 2007),  $\Omega_m = 0.238$ ,  $\Omega_\Lambda = 0.762$ ,  $h = H_0/100 \text{ km s}^{-1} \text{ Mpc}^{-1} = 0.734$ , the spectral index of initial density fluctuations  $n_s = 0.951$  and normalization  $\sigma_8 = 0.744$ .

The iterative criterion (ITER) outlined in Section 3 is applied to select centrals and their satellites from SDSSV. The parameters (a, b, c) in Eq. (11) that define the aperture used in the final iteration of the central-satellite selection are listed in the last row of Table 2. The total number of central galaxies that host at least one satellite is 3863. The number of satellite galaxies selected is 6101.

Fig. 7 shows the scatter plot of the velocity difference,

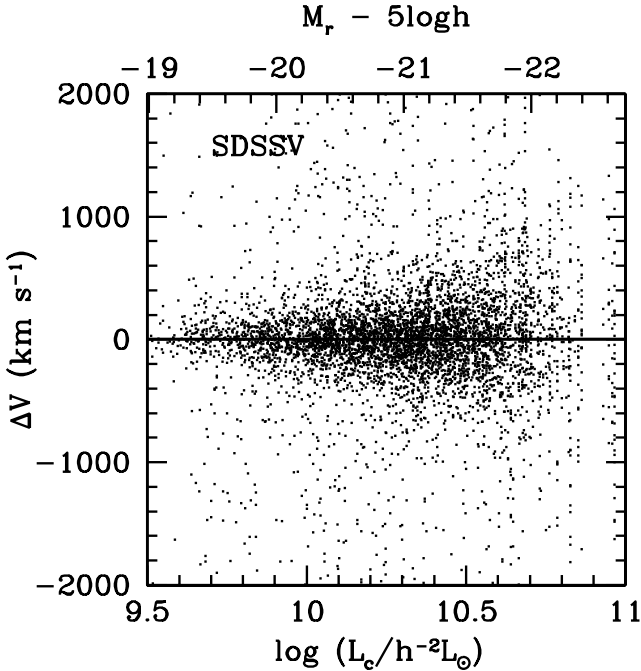


**Figure 7.** Scatter plot of the velocity difference,  $\Delta V$ , between the satellites and their central galaxies as a function of the central galaxy luminosity. The central galaxies and satellites are selected from SDSSV using the iterative selection criterion described in Section 3.

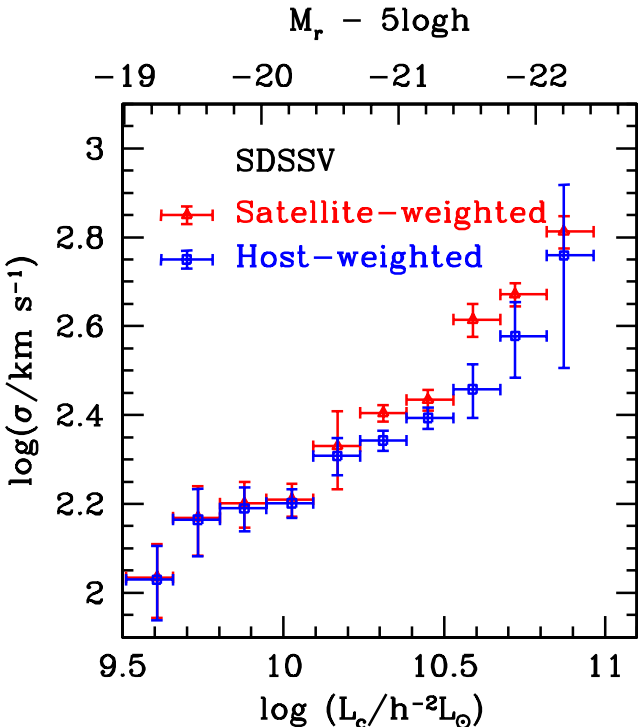


**Figure 8.** The satellite-weighted (red triangles) and the host-weighted (blue squares) velocity dispersions obtained from centrals and satellites selected from SDSSV.

**Table 4.** SDSSV: Velocity Dispersion Measurements

$\log(L_c)$	$\sigma_{\text{sw}}$	$\Delta\sigma_{\text{sw}}$	$\sigma_{\text{hw}}$	$\Delta\sigma_{\text{hw}}$
$h^{-2}L_\odot$	$\text{km s}^{-1}$	$\text{km s}^{-1}$	$\text{km s}^{-1}$	$\text{km s}^{-1}$
9.61	108	20	107	20
9.73	148	26	146	25
9.88	159	19	155	18
10.03	162	14	159	12
10.17	214	43	203	20
10.31	254	11	220	11
10.45	272	15	247	13
10.59	412	35	287	39
10.72	470	28	378	73
10.87	650	54	574	254

The velocity dispersion measurements in the satellite-weighted and host-weighted schemes together with the associated errors.

$\Delta V$ , between the selected satellites and the corresponding centrals as a function of the central luminosity. The scatter in the velocities of satellites with respect to their centrals clearly increases with central galaxy luminosity. To quantify this scatter, we obtain the  $P(\Delta V)$  distributions in both the satellite-weighting and the host-weighting schemes by combining the velocity differences,  $\Delta V$ , of satellites within luminosity bins of uniform width  $\Delta \log[L_c] = 0.15$ . The satellite-weighted and the host-weighted velocity dispersions are estimated from these distributions by fitting a double Gaussian plus constant model as described in Section 4.2. Fig. 8 shows these dispersions as a function of central luminosity. The values of  $\sigma_{\text{sw}}$ ,  $\sigma_{\text{hw}}$  and their associated errors are listed in Table 4. Both the satellite-weighted and the host-weighted velocity dispersions increase with the luminosity of the central galaxy. Note that the satellite-weighted velocity dispersions are systematically higher than the host-weighted velocity dispersions. As is evident from Eqs. (18) and (19), this is a sufficient condition to indicate the presence of scatter in the MLR of central galaxies (see Paper I for a detailed discussion).

The model to infer the MLR of central galaxies from the kinematics requires the radial number density distribution of satellites,  $n_{\text{sat}}(r)$ , as an input. For inferring the MLR from the kinematics measured from MOCKV, we used a model of  $n_{\text{sat}}(r)$  that follows the density distribution of the dark matter in an unbiased manner, i.e.,  $\gamma = \mathcal{R} = 1$  in Eq. (4). However with SDSS, it is not clear what functional form of  $n_{\text{sat}}(r)$  should be used. In fact, various studies have shown that the satellite galaxies are spatially anti-biased with respect to the dark matter (Yang et al. 2005b; Chen 2007a,b). Rather than including  $\gamma$  and  $\mathcal{R}$  as free parameters in our model, we seek to constrain these parameters using the observable  $\Sigma(R|L_c)$ . Fig. 9 shows the projected number density distributions of the selected satellites for the five brightest luminosity bins. As can be seen from Eq. (24), predicting  $\Sigma(R|L_c)$  requires the knowledge of  $P(M|L_c)$ , which is the principle goal of our study. It further also requires the knowledge of  $\langle N_{\text{sat}} \rangle(M)$ . Both these quantities are unknown. We proceed as follows. We use the  $P(M|L_c)$  and  $\langle N_{\text{sat}} \rangle(M)$  from the CLF model of Cacciato et al. (2008) which was also used to populate the mock catalogue. We explore two different

models for  $n_{\text{sat}}(r)$ , one with  $\mathcal{R} = \gamma = 1$ , where the number density distribution of satellites follows the dark matter density distribution, and the other with  $\mathcal{R} = 2$  and  $\gamma = 0$ , where the number density distribution of satellites is spatially anti-biased with respect to the dark matter distribution. The former model is shown as a (black) solid line while the latter with a (red) dotted line in Fig. 9. Clearly, the latter model is favoured by the data. Therefore, we use  $\mathcal{R} = 2$  and  $\gamma = 0$  to specify  $n_{\text{sat}}(r)$  for the analysis of the velocity dispersions to infer the MLR of central galaxies.

Next we use the parametric model described in Section 6.1 and constrain it using the measured velocity dispersions,  $\sigma_{\text{sw}}$  and  $\sigma_{\text{hw}}$ , and the number of satellites per central,  $\langle N_{\text{sat}} \rangle$  as a function of the luminosity of centrals. This allows us to determine both the mean and the scatter of the MLR. Using a MCMC, we recover the mean relations  $\langle \log M \rangle(L_c)$ ,  $\sigma_{\log M}(L_c)$  and  $\langle \log L_c \rangle(M)$ . The 16<sup>th</sup>, 50<sup>th</sup> and the 84<sup>th</sup> percentiles of the distributions of the parameter values that describe the  $P(M|L_c)$  distribution for the central galaxies are listed in Table 5. Fig. 10 is the equivalent of Fig. 6 but for SDSSV. The upper panels show the data used to constrain the parameters and the bottom panels show the confidence levels on the inferred mean and scatter of the MLR. The values of  $\langle \log M \rangle(L_c)$  and  $\sigma_{\log M}(L_c)$  together with their 1- $\sigma$  errors are listed in Table 6.

Clearly the average masses of dark matter haloes increase with central galaxy luminosity, as expected. Interestingly, the scatter in halo masses also increases systematically with the luminosity of the central galaxy. At the bright end, this scatter is roughly half a dex. Therefore, stacking central galaxies by luminosity amounts to stacking haloes that cover a wide range in masses. This justifies the need to account for this scatter in the analysis of the satellite kinematics. Neglecting this scatter leads to an overestimate of the halo mass at a given central luminosity. Most previous studies dealing with satellite kinematics have neglected this scatter which has resulted in a biased estimate of the halo mass-luminosity relationship. As we show in Appendix A, their use of strict selection criteria to identify the centrals and satellites have further biased their estimate of the MLR of central galaxies.

### 7.1 Comparisons with Independent Studies

In a recent study, Cacciato et al. (2008) have constrained the CLF using the abundance and clustering of galaxies in SDSS. They have shown that this CLF is also able to reproduce the galaxy-galaxy lensing signal and is further consistent with the MLR obtained from a SDSS group catalog (Yang, Mo & van den Bosch 2008). It is interesting to compare the results of their study with the results obtained here from satellite kinematics. The solid lines in the bottom panels of Fig. 10 show the mean and the scatter of the MLR obtained using the best-fit CLF model from Cacciato et al. (2008). Clearly, these results are in excellent agreement with the results obtained here using the kinematics of satellite galaxies. Amongst others this provides further support that the halo mass assignment in the SDSS group catalog of Yang et al. (2007) is reliable (Wang et al. 2007b).

Since the mean and scatter of the MLR reflect the physics, and in particular the stochasticity, of galaxy formation, it is interesting to compare the results obtained here

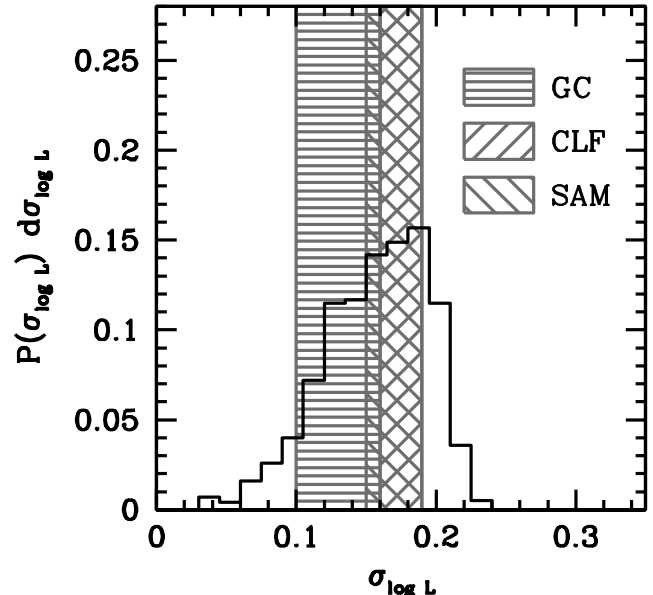


**Figure 11.** The posterior distribution of the parameter  $\sigma_{\log L}$  as obtained from the MCMC analysis of the satellite velocity dispersions. The 1- $\sigma$  constraints on the parameter  $\sigma_{\log L}$  obtained from other independent methods are shown as shaded regions. Region GC indicates the SDSS group catalog result by Yang, Mo & van den Bosch (2008), region CLF indicates the result obtained by Cooray (2006) with an independent CLF analysis and region SAM shows our measurement of  $\sigma_{\log L}$  from the semi-analytical model of Croton et al. (2006).

to predictions from semi-analytical models (SAM) of galaxy formation. To that extent we use the SAM of Croton et al. (2006), which has been shown to match the observed properties of the local galaxy population with reasonable accuracy<sup>1</sup>. Using a volume limited sample of galaxies selected from the SAM with the same luminosity and redshift cuts as SDSSV, we measure the mean and the scatter of the distributions of halo masses for central galaxies in several bins of  $r$ -band luminosity. The results are shown in panels (e) and (f) of Fig. 10 as open squares. The agreement with our constraints from the satellite kinematics is remarkably good. It is both interesting and encouraging that a semi-analytical model, which uses simple, physically motivated recipes to model the complicated baryonic physics associated with galaxy formation, is able to reproduce not only the mean of the MLR of central galaxies but also the correct amount of stochasticity in this relation.

In our model, the stochasticity of galaxy formation is best described by the parameter  $\sigma_{\log L}$ , which indicates the amount of scatter in the luminosity of central galaxies given the mass of a halo, i.e. the scatter in the distribution  $P(L_c|M)$ . The histogram in Fig. 11 shows the posterior probability of  $\sigma_{\log L}$ , obtained from our Monte Carlo Markov Chain, which yields that  $\sigma_{\log L} = 0.16 \pm 0.04$  (68% confidence levels). Note that we have made the assumption that  $\sigma_{\log L}$  is independent of halo mass. The same assumption was made

<sup>1</sup> Note that Croton et al. (2006) adopted a slightly different cosmology than the one used in our data analysis which can have a small impact on the MLR.

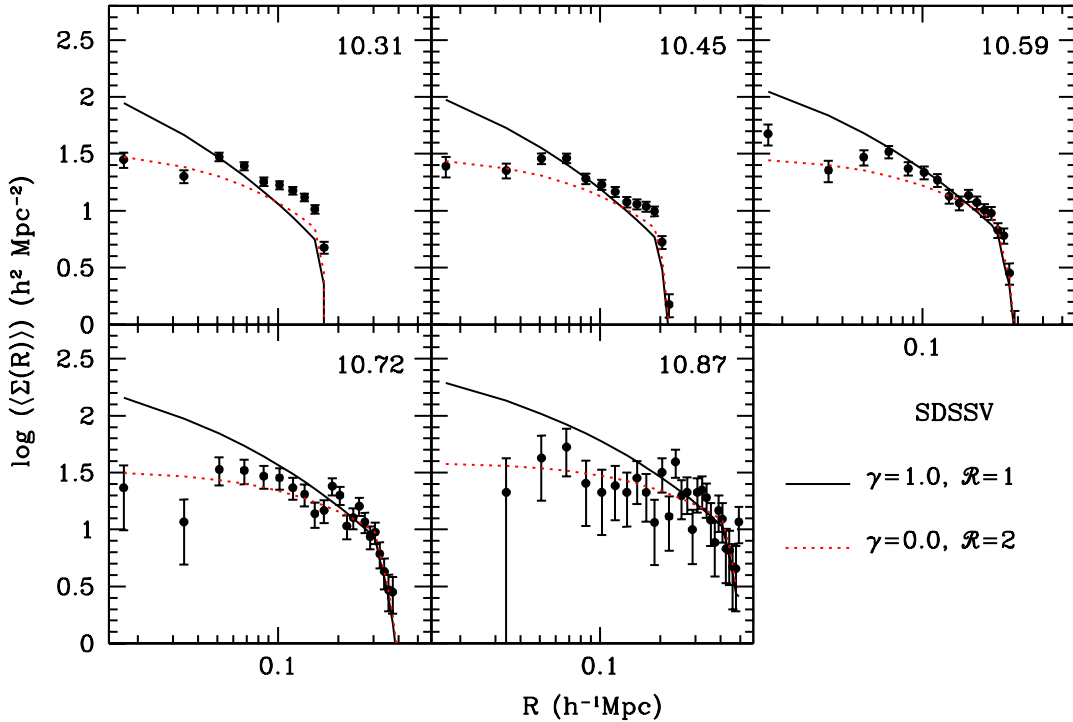


**Figure 9.** The projected number density distributions of satellites around centrals selected from SDSSV for the five bright luminosity bins (average  $\log(L_c/h^{-2}L_\odot)$  in right corner). The (black) solid curves indicate the expected distributions if the number density distribution of satellites follows the dark matter density, i.e.  $\mathcal{R} = \gamma = 1$  in Eq. (4). The (red) dotted curves in turn indicate the expected distributions for a model in which the satellite galaxies are a factor 2 less concentrated than dark matter and have a central core in the number density distribution i.e.  $\mathcal{R} = 2$ , and  $\gamma = 0$ .

by Cooray (2006), who obtained that  $\sigma_{\log L} = 0.17^{+0.02}_{-0.01}$  using the luminosity function and clustering properties of SDSS galaxies (see also Cacciato et al. 2008). Using a large SDSS galaxy group catalogue, Yang, Mo & van den Bosch (2008) obtained direct estimates of the scatter in  $P(L_c|M)$ , and found that  $\sigma_{\log L} = 0.13 \pm 0.03$  with no obvious dependence on halo mass. Finally, we also determined  $\sigma_{\log L}$  in the SAM of Croton et al. (2006): using several bins in halo mass covering the range  $10^{10} h^{-1} M_\odot \leq M \leq 10^{16} h^{-1} M_\odot$ , we find that  $\sigma_{\log L} = 0.17 \pm 0.02$ , once again with virtually no dependence on halo mass. All these results are summarized in Fig. 11. Not only do they support our assumption that  $\sigma_{\log L}$  is independent of halo mass, they also are in remarkable quantitative agreement with each other.

Finally we note that a constant scatter,  $\sigma_{\log L}$ , in the distribution  $P(L_c|M)$  leads to a scatter,  $\sigma_{\log M}(L_c)$ , in the distribution  $P(M|L_c)$  that increases systematically with the luminosity of the central galaxy. This arises from the fact that the relation  $\langle \log L_c \rangle(M)$  (Panel (d) in Fig. 10) is shallower at the high mass end compared to the low mass end (see Paper I).

## 8 SUMMARY

The kinematics of satellite galaxies have been widely used to statistically relate the mean halo masses of central galaxies to their luminosities (Zaritsky et al. 1993; Zaritsky & White 1994; Zaritsky et al. 1997; McKay et al. 2002; Prada et al. 2003; Brainerd & Specian 2003; Norberg et al. 2008).

**Table 5.** SDSSV: Parameters recovered from the MCMC

Parameter	16%	50%	84%
$\log(L_0)$	9.69	10.05	10.33
$\log(M_1)$	10.85	11.74	12.01
$\gamma_2$	0.19	0.28	0.35
$\sigma_{\log L}$	0.12	0.16	0.19

The 16<sup>th</sup>, 50<sup>th</sup> and the 84<sup>th</sup> percentiles of the distributions of parameters that describe the relation  $\tilde{L}_c(M)$  obtained from the MCMC analysis of the velocity dispersions obtained from SDSSV.

These studies use strict criteria to identify central and satellite galaxies that reside preferentially in isolated environments. Following van den Bosch et al. (2004), we applied a relaxed but adaptive selection criterion to a volume limited sample from SDSS to identify centrals and their satellites, not only in isolated environments but also in massive groups and clusters which allowed us to study the kinematics of satellites over a wide range of central galaxy luminosity. We inferred both the mean and the scatter of the mass-luminosity relationship of central galaxies from the kinematics of satellite galaxies.

Using a realistic mock catalogue, we thoroughly tested the analysis method at every step. We tested the performance of our criterion to identify central and satellite galaxies and our method to measure the kinematics of the selected satellites. We showed that the kinematics recovered from the selected satellites are a fair representation of the true kine-

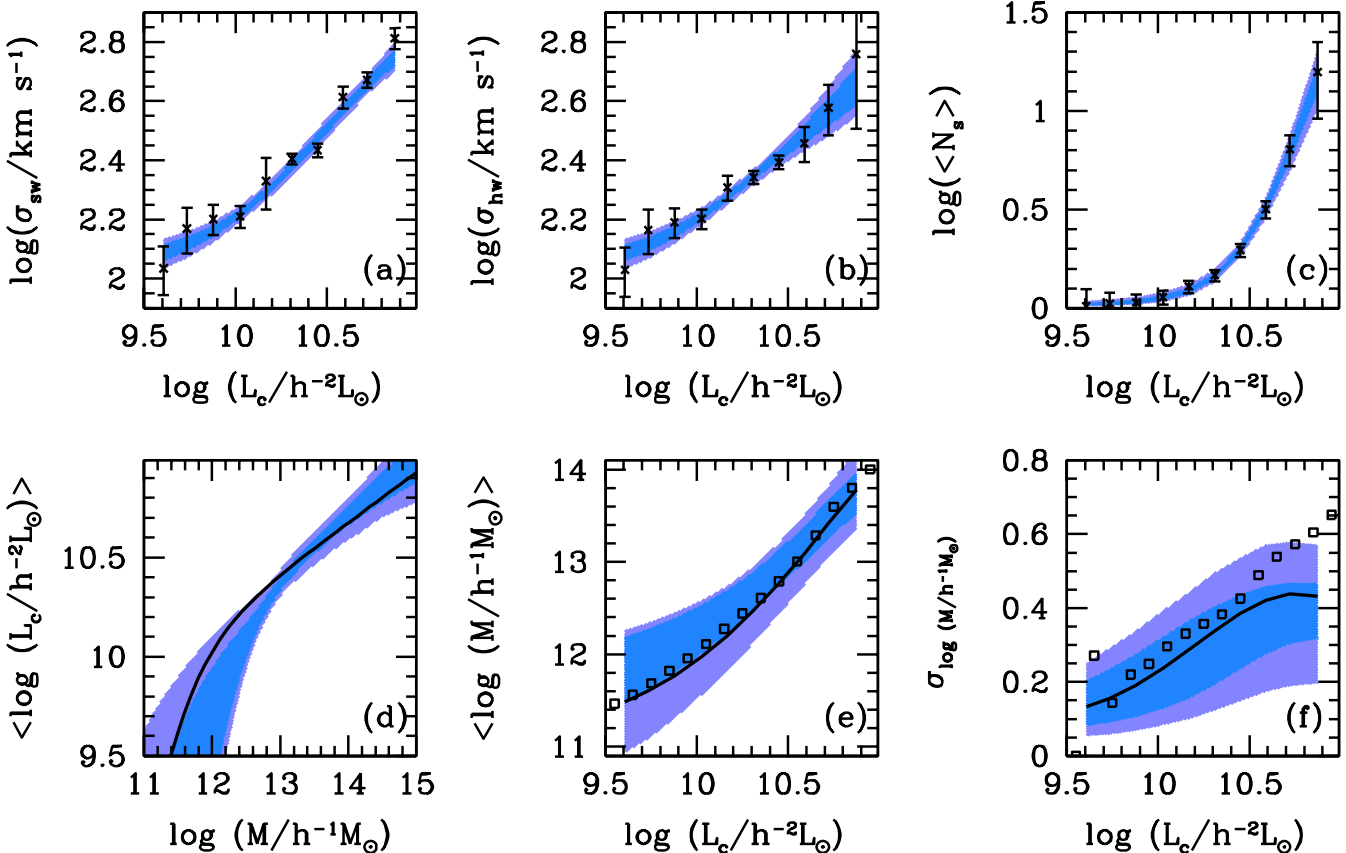


**Figure 10.** Crosses with errorbars in the upper panels show the data points used to constrain the MCMC; the satellite-weighted velocity dispersions in panel (a), the host-weighted velocity dispersions in panel (b) and the mean number of satellites per central as a function of luminosity in panel (c), all measured by using the satellite sample selected from SDSSV. The blue and purple bands represent the 68% and 95% confidence regions respectively. The bottom panels show the relations inferred from the MCMC; the average  $\log(L_c)$  is in panel (d), and the mean and the scatter in the MLR of central galaxies in panels (e) and (f) respectively. The relations obtained by using the halo occupation distribution from MOCKV are shown using solid lines. The squares in panels (e) and (f) indicate the values obtained from the semianalytical model of Croton et al. (2006).

**Table 6.** SDSSV: MLR of Central Galaxies

$\log(L_c)$	$\langle \log M \rangle$	$\Delta \langle \log M \rangle$	$\sigma_{\log M}$	$\Delta \sigma_{\log M}$
$h^{-2}L_\odot$	$h^{-1}M_\odot$	$h^{-1}M_\odot$	$h^{-1}M_\odot$	$h^{-1}M_\odot$
9.61	12.06	0.35	0.12	0.06
9.73	12.16	0.32	0.13	0.07
9.88	12.28	0.29	0.15	0.08
10.03	12.44	0.26	0.18	0.10
10.17	12.60	0.23	0.22	0.10
10.31	12.80	0.21	0.26	0.11
10.45	13.01	0.19	0.30	0.10
10.59	13.24	0.19	0.34	0.09
10.72	13.47	0.21	0.36	0.08
10.87	13.74	0.23	0.38	0.07

The mean and scatter of the halo masses as a function of the central galaxy luminosity inferred from the MCMC analysis. The errors on each of the inferred quantities correspond to the 68% confidence levels.

matics of satellite galaxies present in the mock catalogue. We presented an analytical model that properly accounts for the selection biases and showed that the predictions of

this analytical model are in good agreement with the measured kinematics of the selected satellites.

In Paper I, we have shown that the velocity dispersion of satellites can be measured using two different weighting schemes: satellite-weighting and host-weighting. We have demonstrated a degeneracy between the mean and the scatter of the MLR obtained from either the satellite-weighted or the host-weighted velocity dispersion alone. However, we have also shown that this degeneracy can be broken by using the velocity dispersions in the two schemes simultaneously. In this paper we first tested our method using a mock galaxy catalogue. We fitted the measured satellite-weighted and host-weighted velocity dispersions simultaneously using a parametric model for the halo occupation statistics of central and satellite galaxies, and demonstrated that we can reliably obtain confidence levels on the true mean and scatter of the mass-luminosity relation of central galaxies.

Next we applied the above method to a volume limited sample from the SDSS. The mean of the mass-luminosity relation increases as a function of the central host luminosity indicating that, as expected, more massive haloes host brighter centrals. This result is in excellent quantitative agreement with a recent study by Cacciato et al. (2008),

who use the abundance and clustering properties of galaxies in SDSS to constrain the CLF, and with the SAM of Croton et al. (2006). The satellite kinematics obtained in our study are consistent with a model in which  $P(L_c|M)$  has a constant scatter,  $\sigma_{\log L}$ , independent of the halo mass  $M$ . We obtain  $\sigma_{\log L} = 0.16 \pm 0.04$  in excellent agreement with other independent measurements suggesting that the amount of stochasticity in galaxy formation is similar in haloes of all masses. This is also suggested by the SDSS group catalog of Yang, Mo & van den Bosch (2008) and by the SAM of Croton et al. (2006).

## ACKNOWLEDGMENTS

We are grateful to Kris Blindert, Jacqueline Chen, Anupreeta More, Peder Norberg, Hans-Walter Rix and Joachim Wambsganss for valuable discussion.

## REFERENCES

Adelman-McCarthy J. K., et al., 2006, *ApJS*, 162, 38  
 Becker M. R., et al., 2007, *ApJ*, 669, 905  
 Blanton M. R., et al., 2005, *AJ*, 129, 2562  
 Blumenthal G. R., Faber S. M., Primack J. R., Rees M. J., 1984, *Nat*, 311, 517  
 Brainerd T. G., Specian M. A., 2003, *ApJ*, 593, L7  
 Cacciato M., van den Bosch F. C., More S., Li R., Mo H. J., Yang X., 2008, *MNRAS*, submitted  
 Chen J., 2007a, arXiv, 711, arXiv:0711.0989  
 Chen J., 2007b, arXiv, 712, arXiv:0712.0003  
 Colless M., et al., 2001, *MNRAS*, 328, 1039  
 Conroy C., et al., 2005, *ApJ*, 635, 982  
 Conroy C., et al., 2007, *ApJ*, 654, 153  
 Cooray A., 2006, *MNRAS*, 365, 842  
 Croton D. J., et al., 2006, *MNRAS*, 365, 11  
 Davis M., Efstathiou G., Frenk C. S., White S. D. M., 1985, *ApJ*, 292, 371  
 Diaferio A., Geller M. J., 1996, *ApJ*, 467, 19  
 Erickson L. K., Gottesman S. T., Hunter J. H., Jr., 1987, *Nat*, 325, 779  
 Klypin A., Prada F., 2007, arXiv, 706, arXiv:0706.3554  
 Kravtsov A. V., Berlind A. A., Wechsler R. H., Klypin A. A., Gottlöber S., Allgood B., Primack J. R., 2004, *ApJ*, 609, 35  
 Macciò A. V., Dutton A. A., van den Bosch F. C., Moore B., Potter D., Stadel J., 2007, *MNRAS*, 378, 55  
 McKay T. A., et al., 2002, *ApJ*, 571, L85  
 More S., van den Bosch F. C., Cacciato M., 2008, *MNRAS*, submitted, arXiv:0807.4529  
 Navarro J. F., Frenk C. S., White S. D. M., 1997, *ApJ*, 490, 493  
 Norberg P., Frenk C. S., Cole S., 2008, *MNRAS*, 383, 646  
 Prada F., et al., 2003, *ApJ*, 598, 260  
 Porciani C., Dekel A., Hoffman Y., 2002, *MNRAS*, 332, 325  
 Spergel D. N., et al., 2007, *ApJS*, 170, 377  
 van den Bosch F. C., Norberg P., Mo H. J., Yang X., 2004, *MNRAS*, 352, 1302  
 Wang Y., Yang X., Mo H. J., van den Bosch F. C., 2007a, *ApJ*, 664, 608  
 Wang Y., Yang X., Mo H. J., van den Bosch F. C., Weinmann S. M., Chu Y., 2007b, arXiv, 711, arXiv:0711.4431  
 White S. D. M., Rees M. J., 1978, *MNRAS*, 183, 341  
 Yang X., Mo H. J., Jing Y. P., van den Bosch F. C., 2005a, *MNRAS*, 358, 217  
 Yang X., Mo H. J., van den Bosch F. C., Weinmann S. M., Li C., Jing Y. P., 2005b, *MNRAS*, 362, 711  
 Yang X., Mo H. J., van den Bosch F. C., Pasquali A., Li C., Barden M., 2007, *ApJ*, 671, 153  
 Yang X., Mo H. J., van den Bosch F. C., 2008, *ApJ*, 676, 248  
 York D. G., et al., 2000, *AJ*, 120, 1579  
 Zaritsky D., Smith R., Frenk C., White S. D. M., 1993, *ApJ*, 405, 464  
 Zaritsky D., White S. D. M., 1994, *ApJ*, 435, 599  
 Zaritsky D., Smith R., Frenk C., White S. D. M., 1997, *ApJ*, 478, 39

## APPENDIX A: SAMPLING OF CENTRAL GALAXIES

The ultimate goal of satellite kinematics is to probe the halo mass-luminosity relationship (MLR) of central galaxies. In principle, an unbiased estimate for the MLR requires that the central galaxies identified by the selection criterion are an unbiased (sub-)sample with respect to their corresponding dark matter haloes. In this appendix, we investigate, using the MGC, how our iterative criterion performs in this respect and compare it with the strict criterion used in the literature.

For reasons that will become clear later, we use the flux-limited sample MOCKF for this test. The solid lines in Fig. A1 show the distributions of halo masses,  $P(M|L_c)$ , for all central galaxies in MOCKF divided in 5 luminosity bins. The average logarithm of the luminosities of central galaxies in each bin is indicated at the top right corner. The dotted lines show the distributions,  $P(M|L_c)$ , for all central galaxies that have at least one satellite in the selection aperture defined by our iterative selection criterion. Finally, the histograms show the distributions,  $P(M|L_c)$ , of the centrals selected by our iterative criterion. Clearly, the centrals selected by our iterative criterion sample the distribution of halo masses from the dotted lines (and not the solid lines). However, as discussed in Section 4.3, this bias is taken into account while modelling the kinematics (see Eq. [22]) and therefore allows us to make an unbiased estimate. As shown in Section 6, we indeed recover an unbiased MLR from the kinematics of the selected satellites measured around the centrals selected by our iterative criterion.

For comparison, we now repeat this exercise using the strict criterion employed in previous studies. In particular, we adopt the criterion used in N08. This criterion identifies a galaxy as a central if it is at least  $f_h = 2$  times brighter than any other galaxy in a fixed (irrespective of the luminosity of the galaxy) aperture cylinder (see Table 1) around itself. Satellites are identified as those galaxies that are at least  $f_s = 8$  times fainter than the centrals and reside in a smaller aperture cylinder defined around the centrals. The values of  $f_h$  and  $f_s$  in the N08 criterion are conservative, as the principle goal of their study was to select isolated central galaxies. Applying the N08 criterion to MOCKF selects

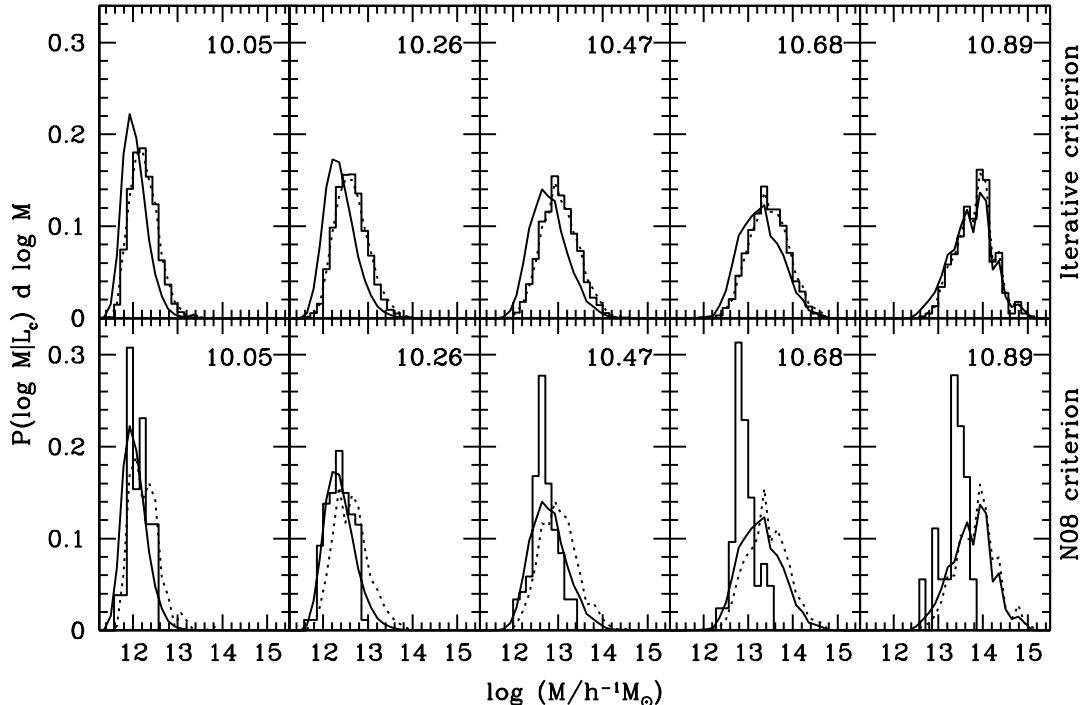


**Figure A1.** Comparison of the sampling of central galaxies using the iterative selection criterion (ITER) used in this paper and the criterion used in Norberg et al. (2008) (N08). The histograms in the upper (bottom) panel show the distributions of halo masses of central galaxies selected according to ITER (N08). The average  $\log(L_c/h^{-2}L_\odot)$  for central galaxies in each bin is indicated at the top right corner of each panel. The solid lines show the true distributions of halo masses for all the central galaxies and the dotted lines show the distribution of halo masses of those central galaxies that have at least one satellite more than  $f_s$  times fainter than themselves in the inner cylinder defined by the selection criterion.

only 126 satellites around 96 central galaxies. Therefore, to do a meaningful comparison, we apply the N08 criterion to MOCKF for which it selects 657 satellites around 395 centrals. For comparison, our iterative criterion yields 39951 satellites around 21206 centrals.

Solid lines in the lower panels of Fig. A1 are the same as in the upper panels and show the distributions of halo masses,  $P(M|L_c)$ , for all central galaxies in MOCKF divided in 5 central luminosity bins. The dotted lines show the  $P(M|L_c)$  for those centrals that have at least one satellite around them which is  $f_s (= 8)$  times fainter than themselves. There is a negligibly small difference in the dotted lines in the two rows due to different values of  $f_s$ . Finally, the histograms show the  $P(M|L_c)$  distributions of the sample of centrals selected by the N08 criterion. Clearly, these do not sample the distributions shown by the dotted lines and the distributions are clearly biased towards the low mass end, especially, in the bright luminosity bins. This owes to the fact that Norberg et al. (2008) adopt  $f_h = 2$ , which preferentially selects centrals that do not have satellite galaxies of comparable brightness. This biases the distributions towards the low mass end. Note, though, that this is not a critique regarding their selection criteria; after all, as Norberg et al. (2008) clearly described in their paper, their principal goal is to study the kinematics around *isolated* galaxies. However, it does mean that it is not meaningful to compare their MLR, which is only applicable to isolated galaxies, to that obtained here, which is representative of the entire central galaxy population.